

Behavior of perturbed plasma displacement near regular and singular X-points for compressible ideal magnetohydrodynamic stability analysis

F. Alladio,^{a)} A. Mancuso, and P. Micozzi

Associazione EURATOM-ENEA sulla Fusione, CR Frascati, C.P. 65-00044, Frascati, Rome, Italy

F. Rogier

ONERA-CERT/DTIM/M2SN 2, avenue Edouard Belin-BP 4025-31055, Toulouse Cedex 4, France

(Received 17 March 2006; accepted 13 June 2006; published online 16 August 2006)

The ideal magnetohydrodynamic (MHD) stability analysis of axisymmetric plasma equilibria is simplified if magnetic coordinates, such as Boozer coordinates (ψ_T radial, i.e., toroidal flux divided by 2π , θ poloidal angle, ϕ toroidal angle, with Jacobian $\sqrt{g} \propto 1/B^2$), are used. The perturbed plasma displacement $\vec{\xi}$ is Fourier expanded in the poloidal angle, and the normal-mode equation $\delta W_p(\vec{\xi}^*, \vec{\xi}) = \omega^2 \delta W_k(\vec{\xi}^*, \vec{\xi})$ (where δW_p and δW_k are the perturbed potential and kinetic plasma energies and ω^2 is the eigenvalue) is solved through a 1D radial finite-element method. All magnetic coordinates are however plagued by divergent metric coefficients, if magnetic separatrices exist within (or at the boundary of) the plasma. The ideal MHD stability of plasma equilibria in the presence of magnetic separatrices is therefore a disputed problem. We consider the most general case of a simply connected axisymmetric plasma, which embeds an internal magnetic separatrix— $\psi_T = \psi_T^X$, with rotational transform $\iota(\psi_T^X) = 0$ and regular X-points ($\vec{B} \neq 0$)—and is bounded by a second magnetic separatrix at the edge— $\psi_T = \psi_T^{\max}$, with $\iota(\psi_T^{\max}) \neq 0$ —that includes a part of the symmetry axis ($R=0$) and is limited by two singular X-points ($\vec{B}=0$). At the embedded separatrix, the ideal MHD stability analysis requires the continuity of the normal plasma perturbed displacement variable, $\xi^\psi = \vec{\xi} \cdot \vec{\nabla} \psi_T$; the other displacement variables, the binormal $\eta^\psi = \vec{\xi} \cdot (\vec{\nabla} \theta - \iota \vec{\nabla} \phi)$ and the parallel $\mu = -\sqrt{g} \vec{\xi} \cdot \vec{\nabla} \phi$, can instead be discontinuous everywhere. The permissible asymptotic limits of $(\xi^\psi, \eta^\psi, \mu)$ are calculated for the unstable ($\omega^2 < 0$) eigenvectors, imposing the regularity of δW_p , δW_k , and $\vec{\xi}$ at the embedded separatrix and at the edge separatrix. An intensified numerical radial mesh following Boozer magnetic coordinates is set up; it requires a logarithmic fit to the rotational transform near the embedded magnetic separatrix, a minimum distance between the radial mesh and both separatrices, and finally an extended spectrum of poloidal mode numbers in the Boozer angle. The numerical results are compared “*a posteriori*” with the permissible asymptotic limits for the perturbed displacement: the radial displacement variable ξ^ψ is found to be always near its most unstable asymptotic limit, while the full range of permissible asymptotic behaviors can be obtained for the binormal and the parallel displacement variables. © 2006 American Institute of Physics. [DOI: 10.1063/1.2220008]

I. INTRODUCTION

When magnetic separatrices are present, the ideal magnetohydrodynamic (MHD) stability analysis of (even axisymmetric) plasma equilibria is a disputed problem. We consider the magnetic configuration of a simply connected axisymmetric plasma, embedding an internal magnetic separatrix— $\psi_T = \psi_T^X$, with vanishing rotational transform, $\iota(\psi_T^X) = 0$ —whose regular X-points ($\vec{B} \neq 0$) join independent tori; an outermost plasma surrounds the first embedded separatrix and is bounded at the edge by a second magnetic separatrix— $\psi_T^{\text{edge}} = \psi_T^{\max}$, with nonvanishing rotational transform, $\iota(\psi_T^{\max}) \neq 0$ —which includes a part of the symmetry axis ($R=0$) and is limited by two singular X-points ($\vec{B}=0$). Such axisymmetric plasma equilibrium, with poloidal flux

$\psi = \int \vec{B} \cdot d\vec{S}_p$ ($\psi=0$ on the symmetry axis of the main torus), normalized toroidal flux $\psi_T = \int \vec{B} \cdot d\vec{S}_T / 2\pi$ ($\psi_T=0$ on the magnetic axis), rotational transform $\iota(\psi_T) = -(d\psi/d\psi_T) / 2\pi$, normalized toroidal current $I(\psi_T) = \int \vec{\nabla} \wedge \vec{B} \cdot d\vec{S}_T / 2\pi$, and normalized poloidal current $f(\psi_T) = \int \vec{\nabla} \wedge \vec{B} \cdot d\vec{S}_p / 2\pi$, can be expressed by nonorthogonal Boozer magnetic coordinates¹ $\{\psi_T = \text{radial coordinate}, \theta = \text{poloidal angle}, \phi = \text{toroidal angle}, \text{with Jacobian } \sqrt{g} = [f(\psi_T) + \iota(\psi_T)I(\psi_T)] / B^2 \text{ and nonorthogonality coefficient } \beta_*(\psi_T, \theta)\}$. The Boozer coordinates were originally invented for charged particles orbit calculations in nonaxisymmetric toroidal magnetic configurations (stellarators); only a few years later the use of these coordinates was found to be particularly expedient for the analysis of ideal MHD stability² of general magnetized plasmas: therefore, they will be used for the latter purpose in this paper. Alternative choices for magnetic coordinates have been consid-

^{a)}Electronic mail: alladio@frascati.enea.it

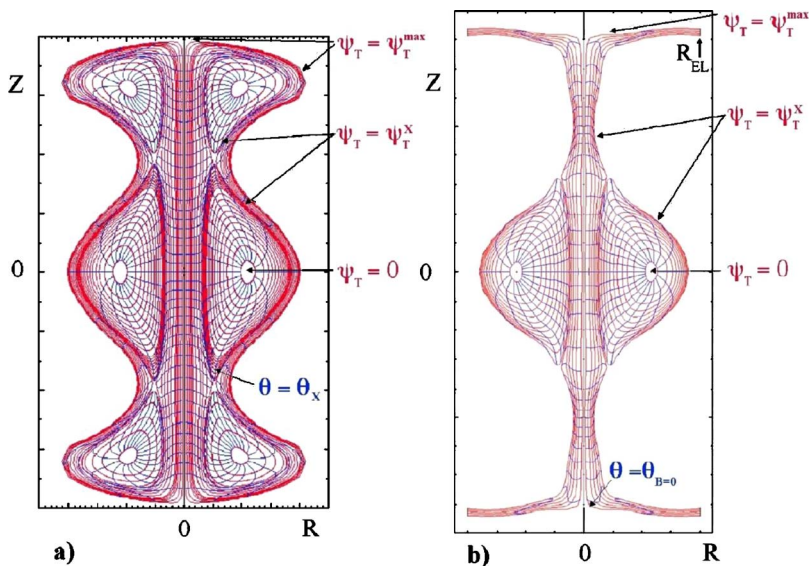


FIG. 1. (Color) Magnetic coordinates for: (a) a CKF configuration, showing a refined radial mesh near the magnetic separatrices and the “central angle” θ_x that labels the lower regular X-point; (b) a FCS configuration, showing the angle $\theta_{B=0}$ that labels the lower singular X-point.

ered, among those already used in other MHD stability analyses. In particular, the Princeton equilibrium, stability, and transport code (PEST) coordinates³ [with $\sqrt{g_{\text{PEST}}} \propto R^2/f(\psi)$] have the advantage that the toroidal angle ϕ_{PEST} coincides with the geometric azimuth φ , but are better avoided for plasma configurations extending up to the symmetry axis, as an artificial singularity $1/R$ would be introduced upon the gradient $\vec{\nabla}\psi_{\text{PEST}}$ of its radial coordinate [$\psi_{\text{PEST}} \propto \int d\psi/f(\psi)$].

A first example of the simply connected axisymmetric configurations considered in this paper is the Chandrasekhar-Kendall-Furth (CKF) (Ref. 4) system [Fig. 1(a)], composed of a main spherical torus (ST, carrying a current with a main toroidal component I_{ST}); two secondary tori (SC, each carrying a current with a main toroidal component I_{SC}) on top and bottom of the main torus; an outermost toroidal shell plasma (SP, carrying a current with a main poloidal component I_e), which extends up to the symmetry axis and surrounds the three tori.

A second example is the “flux-core-spheromak” (FCS) configuration,⁵ or “spherical torus with plasma central column”⁶ (ST-PCC), where the embedded magnetic separatrix divides a spherical torus (ST), which has closed flux surfaces and carries a total toroidal current I_{ST} , from a screw pinch discharge (SP), which has open flux surfaces ending upon electrodes⁷ and carries a (mainly poloidal) plasma electrode current I_e [Fig. 1(b)]. The ambiguity of the definitions of the Boozer coordinates on open flux surfaces has been resolved in a previous paper,⁸ adopting the choices that are most suitable for the computation of the ideal MHD stability of these combined plasmas.

Section II reviews the well-known variational approach⁹ to the normal-mode equation for ideal MHD stability and defines the normal, binormal, and parallel representation¹⁰ of the perturbed displacement in terms of the Boozer coordinates. Section III details the divergences of the metric of these coordinates near the magnetic separatrices. Section IV analyzes the incompressible plasma potential perturbed energy (in a form which is coherent with that introduced by

Cooper¹⁰) and in addition the kinetic and the compressible potential plasma perturbed energies, which were not considered in previous approaches to ideal MHD stability analysis in Boozer coordinates. Section V calculates the permissible asymptotic limits for the perturbed displacement at a regular X-point; Sec. VI undertakes the same task for a singular X-point on the symmetry axis. Focusing on the free-boundary ideal MHD stability calculations for simply connected plasmas, extending up to the symmetry axis, Sec. VII presents the required change of variables, and Sec. VIII integrates the perturbed vacuum energy into the normal-mode equation. Section IX introduces numerical results obtained near the embedded magnetic separatrix. Finally, Sec. X summarizes the paper.

II. ENERGY PRINCIPLE

It is well known that the linearized normal-mode equation, describing the ideal MHD stability of magnetized plasma, can be expressed in a variational form.⁹ Considering the perturbed displacement vector $\vec{\xi}$ away from the equilibrium, with time dependence $e^{i\omega t}$ (its complex conjugate being $\vec{\xi}^*$), the perturbed kinetic energy of plasma with scalar mass density ρ_0 is $\delta W_k(\vec{\xi}^*, \vec{\xi}) = \frac{1}{2} \int V_p dV \rho_0 (\vec{\xi}^* \cdot \vec{\xi})$ and the perturbed potential energy of plasma is $\delta W_p(\vec{\xi}^*, \vec{\xi}) = \frac{1}{2} \int V_p dV \vec{\xi}^* \cdot \vec{F}(\vec{\xi})$, with $\vec{F}(\vec{\xi})$ being the self-adjoint force operator.¹¹ The variational principle states that any function $\vec{\xi}$, which makes stationary the Rayleigh quotient

$$\frac{\delta W_p(\vec{\xi}^*, \vec{\xi})}{\delta W_k(\vec{\xi}^*, \vec{\xi})} = \Omega^2(\vec{\xi}^*, \vec{\xi}) = \omega^2, \quad (1)$$

is an eigenfunction of the normal-mode equation with eigenvalue ω^2 . If the minimum eigenvalue ω^2 is negative, the magnetized plasma is ideally MHD unstable. The relation between the perturbed plasma displacement $\vec{\xi}$, the equilibrium magnetic field \vec{B} , and the perturbed magnetic field \vec{B}_1 is

$$\vec{\mathbf{B}}_1 = \vec{\nabla} \wedge (\vec{\xi} \wedge \vec{\mathbf{B}}). \quad (2)$$

The perturbed potential energy of the plasma, δW_p , is written in a compact form² as

$$\delta W_p = \frac{1}{2} \int_{V_p} dV \left[\frac{|\vec{\mathbf{C}}|^2}{\mu_0} + \Gamma p (\vec{\nabla} \cdot \vec{\xi})^2 - D (\vec{\xi} \cdot \vec{\nabla} \psi_T)^2 \right], \quad (3)$$

with

$$\vec{\mathbf{C}} = \vec{\nabla} \wedge (\vec{\xi} \wedge \vec{\mathbf{B}}) + \mu_0 \frac{(\vec{\mathbf{j}} \wedge \vec{\nabla} \psi_T)}{|\vec{\nabla} \psi_T|^2} \vec{\xi} \cdot \vec{\nabla} \psi_T \quad (4)$$

and

$$D = 2 \frac{(\vec{\mathbf{j}} \wedge \vec{\nabla} \psi_T)}{|\vec{\nabla} \psi_T|^2} \cdot (\vec{\mathbf{B}} \cdot \vec{\nabla}) \left(\frac{\vec{\nabla} \psi_T}{|\vec{\nabla} \psi_T|^2} \right), \quad (5)$$

where p is the kinetic plasma pressure, $\vec{\mathbf{j}}$ is the equilibrium current density ($\vec{\mathbf{j}} \wedge \vec{\mathbf{B}} = \vec{\nabla} p$), and Γ is the adiabatic index (usually set to $\Gamma = 5/3$). The perturbed displacement $\vec{\xi}$ is expressed¹⁰ in terms of the normal ξ^ψ , binormal η^ψ , and parallel μ displacement variables as follows:

$$\vec{\xi} = \xi^\psi \vec{\mathbf{e}}_\psi + \eta^\psi \frac{\vec{\mathbf{B}} \wedge \vec{\nabla} \psi_T}{B^2} + \left(\frac{I \eta^\psi}{B^2} - \mu \right) \vec{\mathbf{B}}, \quad (6)$$

where $\vec{\mathbf{e}}_\psi$ is the Boozer covariant radial basis vector.⁸ Whereas ξ^ψ is directly the Boozer normal contravariant component of $\vec{\xi}$, η^ψ and μ are defined in terms of the other contravariant components of $\vec{\xi}$,

$$\xi^\psi = \vec{\xi} \cdot \vec{\nabla} \psi_T, \quad (7)$$

$$\eta^\psi = \vec{\xi} \cdot (\vec{\nabla} \theta - \epsilon \vec{\nabla} \phi) = \xi^\theta - \epsilon \xi^\phi, \quad (8)$$

$$\mu = -\sqrt{g} \vec{\xi} \cdot \vec{\nabla} \phi = -\sqrt{g} \xi^\phi. \quad (9)$$

The $(\xi^\psi, \eta^\psi, \mu)$ description provides simple expressions for the contravariant components of the perturbed magnetic field (2),

$$B_1^\psi = [\vec{\nabla} \wedge (\vec{\xi} \wedge \vec{\mathbf{B}})]^\psi = \frac{1}{\sqrt{g}} \left[\epsilon \frac{\partial \xi^\psi}{\partial \theta} + \frac{\partial \xi^\psi}{\partial \phi} \right] = \vec{\mathbf{B}} \cdot \vec{\nabla} \xi^\psi, \quad (10)$$

$$B_1^\theta = [\vec{\nabla} \wedge (\vec{\xi} \wedge \vec{\mathbf{B}})]^\theta = \frac{1}{\sqrt{g}} \left[\frac{\partial \eta^\psi}{\partial \phi} - \frac{\partial (\epsilon \xi^\psi)}{\partial \psi_T} \right], \quad (11)$$

$$B_1^\phi = [\vec{\nabla} \wedge (\vec{\xi} \wedge \vec{\mathbf{B}})]^\phi = \frac{1}{\sqrt{g}} \left[-\frac{\partial \eta^\psi}{\partial \theta} - \frac{\partial \xi^\psi}{\partial \psi_T} \right]. \quad (12)$$

A remarkable property is that neither the parallel variable μ nor the radial derivative of the binormal variable $\partial \eta^\psi / \partial \psi_T$, enters the perturbed magnetic field (10)–(12). The parallel variable μ contributes to δW_p (3) only through the plasma compression term,

$$\delta W_p^c = \frac{\Gamma}{2} \int_{V_p} dV p (\vec{\nabla} \cdot \vec{\xi})^2, \quad (13)$$

which is positive definite and so stabilizing. Therefore, it would be easier to calculate the incompressible ($\vec{\nabla} \cdot \vec{\xi} = 0$) ideal MHD stability in terms of just two variables: ξ^ψ and η^ψ . In this case μ would be determined, after solving the normal-mode equations (1), from the magnetic differential equation:² $\sqrt{g} \vec{\mathbf{B}} \cdot \vec{\nabla} \mu = \partial(\sqrt{g} \xi^\psi) / \partial \psi_T + \partial(\sqrt{g} \eta^\psi) / \partial \theta$. The incompressibility constraint would eliminate the displacement variable μ from the problem without affecting the marginal stability, while the calculated eigenfunctions and growth rates would not be correct anymore. But, the analysis of the plasma perturbations near the regular (Sec. V) and the singular X -points (Sec. VI) shows that, in case of divergence, the binormal and parallel displacement variables, η^ψ and μ , compensate each other. Furthermore, this analysis will be extended, in a forthcoming paper, to axisymmetric instabilities (with toroidal mode number $n=0$); those modes have the feature that $\vec{\nabla} \cdot \vec{\xi} = 0$ is not a suitable condition; their parallel displacement variable μ is instead determined, in terms of ξ^ψ and η^ψ , by the vanishing of the covariant component of the perturbed displacement,¹² $\xi_\phi = \vec{\xi} \cdot \vec{\mathbf{e}}_\phi = R \vec{\xi} \cdot \hat{\mathbf{e}}_\phi = 0$, where $\vec{\mathbf{e}}_\phi$ is the Boozer covariant toroidal basis vector⁸ and $\hat{\mathbf{e}}_\phi$ the unit vector along the geometrical azimuth ϕ . It seems therefore better to avoid the incompressibility simplification and to maintain the fully compressible energy principle for the analysis of perturbed plasma displacements near X -points.

III. DIVERGENCES OF MAGNETIC COORDINATES NEAR SEPARATRICES

The main results of a recent paper⁸ are summarized here, for the convenience of the reader. At the embedded magnetic separatrix ($\psi_T = \psi_T^X$) the rotational transform vanishes as $\lim_{\psi_T \rightarrow \psi_T^X} \epsilon(\psi_T) \propto 1/|\ln|\psi_T^X - \psi_T||$, while its derivative with respect to the radial Boozer coordinate diverges. The component of $\vec{\nabla} \theta$ upon the flux surfaces, approaching the separatrix, diverges near the regular X -point ($\vec{\mathbf{B}} \neq 0$) as $1/\sqrt{|\psi_T^X - \psi_T|} \sqrt{|\ln|\psi_T^X - \psi_T||}$, implying that, although the Boozer poloidal angles θ have to converge there, each regular X -point can be labeled by its ‘‘central angle’’ θ_X [see Fig. 1(a)]. The ‘‘integrated residual shear’’ $\gamma_*(\psi_T, \theta) = \vec{\nabla} \psi_T \cdot (\vec{\nabla} \theta - \epsilon \vec{\nabla} \phi) / |\vec{\nabla} \psi_T|^2$ diverges radially near the X -point ($\theta \rightarrow \theta_X$) as $1/|\psi_T^X - \psi_T| |\ln|\psi_T^X - \psi_T||$, corresponding to $|\vec{\nabla} \psi_T|^2$ vanishing as $|\psi_T^X - \psi_T| |\ln|\psi_T^X - \psi_T||$, and vanishes far from the X -point [$|\theta - \theta_X| \sim O(1)$] as $1/|\ln|\psi_T^X - \psi_T||^2$, corresponding to $|\vec{\nabla} \psi_T|^2$ diverging as $|\ln|\psi_T^X - \psi_T||^2$.

At the edge magnetic separatrix ($\psi_T^{\text{edge}} = \psi_T^{\text{max}}$) the rotational transform ϵ is instead finite: $\lim_{\psi_T \rightarrow \psi_T^{\text{max}}} \epsilon(\psi_T) = \epsilon_{\text{symm}} \neq 0$.

Near the singular X -points, using local spherical coordinates (r, ϑ, φ) , the magnetic field vanishes as $B \propto r$, $|\vec{\nabla} \psi_T|$ vanishes as r^2 , the integrated residual shear γ_* diverges as $1/r$ (while being regular far from the singular X -points) and the compo-

ment of $\vec{\nabla}\theta$ upon the flux surfaces vanishes as r ; this explains why no convergence of poloidal Boozer angles θ occurs into the singular X -points, the lower of which is therefore uniquely labeled by the poloidal angle $\theta_{B=0}$ [see Fig. 1(b)].

A number of metric coefficients, defined as dot products between the covariant basis vectors: $g_{ij} = \vec{e}_i \cdot \vec{e}_j$, and some among their radial and poloidal derivatives furthermore diverge:

- At the embedded magnetic separatrix, near a regular X -point:

$$\lim_{\psi_T \rightarrow \psi_T^X, \theta \rightarrow \theta_X} g_{\psi\psi} \propto 1/|\psi_T^X - \psi_T| |\ln|\psi_T^X - \psi_T||;$$

far from a regular X -point:

$$\lim_{\psi_T \rightarrow \psi_T^X, |\theta - \theta_X| \sim O(1)} g_{\theta\theta} \propto |\ln|\psi_T^X - \psi_T||^2$$

and

$$\lim_{\psi_T \rightarrow \psi_T^X, |\theta - \theta_X| \sim O(1)} g_{\theta\phi} \propto |\ln|\psi_T^X - \psi_T||.$$

- At the plasma edge, near a singular X -point

$$\lim_{\psi_T \rightarrow \psi_T^{\max}, \theta \rightarrow \theta_{B=0}} g_{\psi\psi} \propto 1/r^4,$$

$$\lim_{\psi_T \rightarrow \psi_T^{\max}, \theta \rightarrow \theta_{B=0}} \sqrt{g} \propto 1/r^2$$

and

$$\lim_{\psi_T \rightarrow \psi_T^{\max}, \theta \rightarrow \theta_{B=0}} g_{\theta\theta} \propto 1/r^2,$$

where r is the distance from the singular X -point. This means that the derivatives of the Jacobian with respect to the Boozer coordinates diverge as $\partial\sqrt{g}/\partial\psi_T \propto 1/r^5$ and $\partial\sqrt{g}/\partial\theta \propto 1/r^4$.

- On the symmetry axis ($\psi_T = \psi_T^{\max}$ and $R=0$), where $\vec{\nabla}\psi_T$ vanishes: $\lim_{R \rightarrow 0} |\vec{\nabla}\psi_T| \propto R$, the only diverging metric coefficient is $\lim_{R \rightarrow 0} g_{\psi\psi} \propto 1/R^2$.

IV. THE COMPRESSIBLE PERTURBED ENERGIES

The incompressible part of the perturbed potential energy of the plasma $\delta W_p^i = \delta W_p - \delta W_p^c$, when written in terms of the $(\xi^\psi, \eta^\psi, \mu)$ representation, becomes a quadratic form in the variable ξ^ψ and in the derivatives $\partial\xi^\psi/\partial\psi_T$, $\epsilon\partial\xi^\psi/\partial\theta + \partial\xi^\psi/\partial\phi$, $\partial\eta^\psi/\partial\theta$, $\partial\eta^\psi/\partial\phi$. The relevant metric coefficients⁸ are \sqrt{g} , $\partial(\sqrt{g})/\partial\psi_T$, $g_{\psi\psi}$, $g_{\psi\theta}$, $|\vec{\nabla}\psi_T|^2$ and the nonorthogonality coefficient β_* , whereas $g_{\psi\phi} = \sqrt{g}\beta_* - \epsilon g_{\psi\theta}$. After all the simplifications have been performed,¹⁰ in order to single out the parallel plasma current density $(\vec{j} \cdot \vec{B})/B^2$ and the plasma pressure gradient $dp(\psi_T)/d\psi_T$ —which are the two terms driving the ideal MHD instabilities—the quadratic form becomes

$$\begin{aligned} \delta W_p^i = & \frac{1}{2\mu_0} \int_0^{\psi_T^{\text{dge}}} d\psi_T \int_0^{2\pi} d\phi \int_{\theta_{\min}}^{\theta_{\max}} d\theta \left\{ [\sqrt{g}B^2] \left(\frac{\partial\xi^\psi}{\partial\psi_T} \right)^2 - 2[\beta_*] \left(\frac{\partial\xi^\psi}{\partial\psi_T} \right) \left(\epsilon \frac{\partial\xi^\psi}{\partial\theta} + \frac{\partial\xi^\psi}{\partial\phi} \right) + 2 \left[I \left(\frac{d\epsilon}{d\psi_T} \right) + \sqrt{g} \left(\mu_0 \frac{dp}{d\psi_T} \right) \right] (\xi^\psi) \right. \\ & \times \left(\frac{\partial\xi^\psi}{\partial\psi_T} \right) - [2] \left(-f \frac{\partial\eta^\psi}{\partial\theta} + I \frac{\partial\eta^\psi}{\partial\phi} \right) \left(\frac{\partial\xi^\psi}{\partial\psi_T} \right) + \left[\frac{g_{\psi\psi}}{\sqrt{g}} \right] \left(\epsilon \frac{\partial\xi^\psi}{\partial\theta} + \frac{\partial\xi^\psi}{\partial\phi} \right) - 2 \left[\frac{g_{\psi\theta}}{\sqrt{g}} \left(\frac{d\epsilon}{d\psi_T} \right) \right] (\xi^\psi) \left(\epsilon \frac{\partial\xi^\psi}{\partial\theta} + \frac{\partial\xi^\psi}{\partial\phi} \right) \\ & + [2] \left(\frac{g_{\psi\theta}}{\sqrt{g}} \frac{\partial\eta^\psi}{\partial\phi} - \frac{g_{\psi\phi}}{\sqrt{g}} \frac{\partial\eta^\psi}{\partial\theta} \right) \left(\epsilon \frac{\partial\xi^\psi}{\partial\theta} + \frac{\partial\xi^\psi}{\partial\phi} \right) + 2 \left[\left(\mu_0 \frac{(\vec{j} \cdot \vec{B})}{B^2} \right) - \frac{|\vec{\nabla}\psi_T|^2}{\sqrt{g}B^2} \left(\frac{d\epsilon}{d\psi_T} \right) \right] (\xi^\psi) \left(\epsilon \frac{\partial\eta^\psi}{\partial\theta} + \frac{\partial\eta^\psi}{\partial\phi} \right) \\ & - \frac{2}{\sqrt{g}B^2} \left[I \left(\frac{d\epsilon}{d\psi_T} \right) + \sqrt{g} \left(\mu_0 \frac{dp}{d\psi_T} \right) \right] (\xi^\psi) \left(-f \frac{\partial\eta^\psi}{\partial\theta} + I \frac{\partial\eta^\psi}{\partial\phi} \right) + \left[\frac{1}{\sqrt{g}B^2} \right] \left(-f \frac{\partial\eta^\psi}{\partial\theta} + I \frac{\partial\eta^\psi}{\partial\phi} \right)^2 + \left[\frac{|\vec{\nabla}\psi_T|^2}{\sqrt{g}B^2} \right] \left(\epsilon \frac{\partial\eta^\psi}{\partial\theta} + \frac{\partial\eta^\psi}{\partial\phi} \right)^2 \\ & + \left[- \left(\mu_0 \frac{(\vec{j} \cdot \vec{B})}{B^2} \right) \left(\frac{d\epsilon}{d\psi_T} \right) + \left(\frac{d\epsilon}{d\psi_T} \right)^2 \left(\frac{I^2}{\sqrt{g}B^2} + \frac{|\vec{\nabla}\psi_T|^2}{\sqrt{g}B^2} \right) + \left(\mu_0 \frac{dp}{d\psi_T} \right) \left(\frac{\sqrt{g}I}{\sqrt{g}B^2} \left[\frac{d\epsilon}{d\psi_T} \right] + \frac{\partial(\sqrt{g})}{\partial\psi_T} \right) \right] (\xi^\psi)^2 \left. \right\}. \end{aligned} \quad (14)$$

For FCS configurations, with open flux surfaces ending upon electrodes^{6,7} at $\theta_{\min} = \theta_{\text{EL}}(\psi_T)$, $\theta_{\max} = 2\pi - \theta_{\text{EL}}(\psi_T)$, the extremes of integration for the poloidal angle are

$$\theta_{\min} = 0, \quad \theta_{\max} = 2\pi, \quad (15)$$

for the closed flux surfaces in the radial ST range ($0 < \psi_T < \psi_T^X$) and

$$\theta_{\min} = \theta_{\text{EL}}(\psi_T), \quad \theta_{\max} = 2\pi - \theta_{\text{EL}}(\psi_T), \quad (16)$$

for the open flux surfaces in the radial SP range [$\psi_T^X < \psi_T < \psi_T^{\text{dge}} = \psi_T^{\max}$; see Fig. 1(b)].

In axisymmetry the toroidal mode number n is separable; therefore, for any given n , the displacement variables $(\xi^\psi, \eta^\psi, \mu)$ are expanded in a Fourier series of modes with poloidal numbers m_ℓ ,

$$\xi^\psi = \sum_\ell \xi_\ell(\psi_T) \sin(m_\ell \theta - n\phi), \quad (17)$$

$$\eta^\psi = \sum_\ell \eta_\ell(\psi_T) \cos(m_\ell \theta - n\phi), \quad (18)$$

$$\mu = \sum_\ell \mu_\ell(\psi_T) \cos(m_\ell \theta - n\phi). \quad (19)$$

The reduction to a sine component for ξ^ψ and to a cosine component for η^ψ and μ is permitted if up-down symmetric equilibria are assumed (as in this paper; see Fig. 1); in general sine and cosine components for all the displacement variables should be included. The choice of the angular dependence ($m_\ell \theta - n\phi$) is in accordance with the choice of directions¹ for the Boozer coordinates and corresponds to the requirement of accounting for the most unstable modes (the ones with wave vector \vec{k} such that $\vec{k} \cdot \vec{B} \approx 0$, or $\epsilon(m_\ell m_\ell - n \approx 0)$ with positive mode numbers m_ℓ and n). By using the Fourier expansion, the incompressible potential plasma energy is expressed in Appendix A as a quadratic form in the variables ξ_ℓ and η_ℓ and in the radial derivative $\partial \xi_\ell / \partial \psi_T$. The coefficients $C_{\ell\ell}^{(i)}(\psi_T)$ (with $i=0, 1, \dots, 7$) of this form, written

in Appendix A, are poloidal contour integrals expressing the coupling between poloidal mode numbers m_ℓ and $m_{\ell'}$; they are consistent with and ordered as in the paper by Cooper.¹⁰ Most of them exhibit a discontinuity at the embedded magnetic separatrix ($\psi_T = \psi_T^X$); as an example, for a FCS configuration the integrals $C_{\ell\ell}^{(0)}(\psi_T)$ are unitary and purely diagonal inside the ST: $C_{\ell\ell}^{(0)}(\psi_T) = \delta_{m_\ell m_{\ell'}}$ for $0 < \psi_T < \psi_T^X$; they are instead neither unitary nor diagonal inside the SP: $C_{\ell\ell}^{(0)}(\psi_T) = -(1/\pi) [\sin(m_\ell - m_{\ell'}) \theta_{EL}(\psi_T) / (m_\ell - m_{\ell'})]$ for $\psi_T^X < \psi_T < \psi_T^{\max}$. Also, in the case of the CKF configurations,⁴ the coefficients $C_{\ell\ell}^{(i)}(\psi_T)$ are discontinuous at the embedded magnetic separatrix ($\psi_T = \psi_T^X$), as their integration path on the innermost SP flux surface changes suddenly with respect to the outermost ST flux surface, as it has to surround also the two secondary tori [Fig. 1(a)].

The compressible perturbed kinetic energy of the plasma δW_k assumes as mass density the scalar $\rho_0(\psi_T)$; when written in terms of the $(\xi^\psi, \eta^\psi, \mu)$ variables, it becomes a quadratic form; the relevant metric coefficients⁸ are \sqrt{g} , the nonorthogonality coefficient β_* and the integrated residual shear γ_* ,

$$\begin{aligned} \delta W_k = & \frac{1}{2} \int_0^{\psi_T^{\text{edge}}} d\psi_T \rho_0(\psi_T) \int_0^{2\pi} d\phi \int_{\theta_{\min}}^{\theta_{\max}} d\theta \sqrt{g} \left\{ \left[\frac{1}{|\vec{\nabla}\psi_T|^2} + \frac{\beta_*^2}{B^2} + \frac{\gamma_*^2 |\vec{\nabla}\psi_T|^2}{B^2} \right] (\xi^\psi)^2 + \left[\frac{|\vec{\nabla}\psi_T|^2}{B^2} + \frac{I^2}{B^2} \right] (\eta^\psi)^2 + [B^2](\mu)^2 - 2[I] \right. \\ & \left. \times (\eta^\psi)(\mu) + 2 \left[\frac{I\beta_*}{B^2} - \frac{\gamma_* |\vec{\nabla}\psi_T|^2}{B^2} \right] (\xi^\psi)(\eta^\psi) - 2[\beta_*](\xi^\psi)(\mu) \right\}. \quad (20) \end{aligned}$$

The compressible part (13) of the perturbed potential energy of the plasma δW_p^c , when written in terms of the $(\xi^\psi, \eta^\psi, \mu)$ representation, becomes a quadratic form in the variables ξ^ψ and η^ψ and in the derivatives $\partial \xi^\psi / \partial \psi_T$, $\partial \eta^\psi / \partial \theta$ and $\epsilon \partial \mu / \partial \theta + \partial \mu / \partial \phi$; the relevant metric coefficients are \sqrt{g} , $\partial(\sqrt{g}) / \partial \psi_T$, and $\partial(\sqrt{g}) / \partial \theta$,

$$\begin{aligned} \delta W_p^c = & \frac{\Gamma}{2} \int_0^{\psi_T^{\text{edge}}} d\psi_T p(\psi_T) \int_0^{2\pi} d\phi \int_{\theta_{\min}}^{\theta_{\max}} d\theta \left\{ [\sqrt{g}] \left(\frac{\partial \xi^\psi}{\partial \psi_T} \right)^2 + \left[\frac{1}{\sqrt{g}} \left(\frac{\partial(\sqrt{g})}{\partial \psi_T} \right)^2 \right] (\xi^\psi)^2 + \left[2 \frac{\partial(\sqrt{g})}{\partial \psi_T} \right] (\xi^\psi) \left(\frac{\partial \xi^\psi}{\partial \psi_T} \right) + \left[\frac{1}{\sqrt{g}} \left(\frac{\partial(\sqrt{g})}{\partial \theta} \right)^2 \right] \right. \\ & \times (\eta^\psi)^2 + [\sqrt{g}] \left(\frac{\partial \eta^\psi}{\partial \theta} \right)^2 + \left[2 \frac{\partial(\sqrt{g})}{\partial \theta} \right] (\eta^\psi) \left(\frac{\partial \eta^\psi}{\partial \theta} \right) + \left[\frac{1}{\sqrt{g}} \right] \left(\epsilon \frac{\partial \mu}{\partial \theta} + \frac{\partial \mu}{\partial \phi} \right)^2 - \left[\frac{2}{\sqrt{g}} \frac{\partial(\sqrt{g})}{\partial \psi_T} \right] (\xi^\psi) \left(\epsilon \frac{\partial \mu}{\partial \theta} + \frac{\partial \mu}{\partial \phi} \right) - [2] \left(\frac{\partial \xi^\psi}{\partial \psi_T} \right) \\ & \times \left(\epsilon \frac{\partial \mu}{\partial \theta} + \frac{\partial \mu}{\partial \phi} \right) + \left[\frac{2}{\sqrt{g}} \frac{\partial(\sqrt{g})}{\partial \psi_T} \frac{\partial(\sqrt{g})}{\partial \theta} \right] (\eta^\psi)(\xi^\psi) + \left[2 \frac{\partial(\sqrt{g})}{\partial \psi_T} \right] \left(\frac{\partial \eta^\psi}{\partial \theta} \right) (\xi^\psi) + \left[2 \frac{\partial(\sqrt{g})}{\partial \theta} \right] (\eta^\psi) \left(\frac{\partial \xi^\psi}{\partial \psi_T} \right) + [2\sqrt{g}] \left(\frac{\partial \xi^\psi}{\partial \psi_T} \right) \left(\frac{\partial \eta^\psi}{\partial \theta} \right) \\ & \left. - \left[\frac{2}{\sqrt{g}} \frac{\partial(\sqrt{g})}{\partial \theta} \right] \left(\epsilon \frac{\partial \mu}{\partial \theta} + \frac{\partial \mu}{\partial \phi} \right) (\eta^\psi) - [2] \left(\epsilon \frac{\partial \mu}{\partial \theta} + \frac{\partial \mu}{\partial \phi} \right) \left(\frac{\partial \eta^\psi}{\partial \theta} \right) \right\}. \quad (21) \end{aligned}$$

The extremes of integration for the poloidal angle are again (15) and (16). By using the Fourier expansions (17)–(19), the compressible perturbed plasma kinetic energy δW_k and the compressible part δW_p^c of the perturbed plasma potential energy are expressed, respectively, in Appendix B and in Appendix C, as quadratic forms in the displacement variables ξ_ℓ , η_ℓ , μ_ℓ , and in the radial derivative $\partial \xi_\ell / \partial \psi_T$. Most of the

coefficients $K_{\ell\ell}^{(i)}(\psi_T)$ (with $i=0, 1, \dots, 8$) and $D_{\ell\ell}^{(i)}(\psi_T)$ (with $i=0, 1, \dots, 9$) of these quadratic forms exhibit discontinuities at the embedded magnetic separatrix ($\psi_T = \psi_T^X$). As a matter of fact, even if a continuous toroidal current density distribution is enforced, by assuming that the radial derivatives of the plasma pressure $dp(\psi_T)/d\psi_T$ and of the normalized poloidal plasma current $df(\psi_T)/d\psi_T$ are continuous, an

unavoidable source of discontinuity is the divergent radial derivative $d\epsilon(\psi_T)/d\psi_T$ of the rotational transform, which even changes sign at the ST-SP interface. This feature implies that there cannot be continuous ideal MHD stability eigenfunctions, defined over the whole configuration. The discontinuity of the normal perturbed displacement $\vec{\xi} \cdot \vec{\nabla} \psi_T / |\vec{\nabla} \psi_T| = \xi^\psi / |\vec{\nabla} \psi_T|$ at the ST-SP interface is forbidden¹³ in ideal MHD because it would give rise to flux generation and would provide an unavoidable divergence of the perturbed plasma potential energy. On the other hand, discontinuities of the tangential displacement variables (η^ψ, μ) can be allowed everywhere.¹³

V. PERMISSIBLE ASYMPTOTIC LIMITS FOR THE PERTURBED DISPLACEMENT AT A REGULAR X-POINT

Addressing the problem of global ideal MHD instabilities—for low toroidal mode numbers perturbations, $n \leq 3$ —some ideal MHD stability codes¹⁴ have adopted two-dimensional finite elements, still aligned with the flux surfaces, either all over the mesh or just near the magnetic separatrix, in order to avoid the singularities connected with the magnetic separatrices. The approach taken with the STABLE code is instead that of maintaining the 1D radial finite elements: an intensified numerical radial mesh following Boozer magnetic coordinates is set up near the magnetic separatrices; it requires: a logarithmic fit⁸ to the rotational transform just near the embedded magnetic separatrix; a minimum distance between the radial mesh and both separatrices; and finally an extended spectrum of poloidal mode numbers for both separatrices. The numerical results of STABLE are compared *a posteriori* with the permissible asymptotic limits for the perturbed displacement. The prescriptions upon the displacement variables (ξ^ψ, η^ψ, μ) at the two magnetic separatrices are that the potential and kinetic perturbed energies (δW_p and δW_k) do not diverge and that the plasma displacement $\vec{\xi}$ is regular. As a matter of fact, the logarithmic dependence⁸ $\lim_{\psi_T \rightarrow \psi_T^X} \epsilon(\psi_T) \propto 1/\ln|\psi_T^X - \psi_T|$ of the rotational transform near the embedded separatrix creates the asymptotic limit to the perturbed displacement $\vec{\xi}$, while the vanishing of the magnetic field $\lim_{\psi_T \rightarrow \psi_T^{\max}, \theta \rightarrow \theta_{B=0}} \vec{B} \propto r$ plays the same role near the singular X-point at the edge separatrix.

The term $\propto (d\epsilon/d\psi_T)^2 |\vec{\nabla} \psi_T|^2 (\xi^\psi)^2$ of δW_p^i [Eq. (14)] shows that the normal displacement variable ξ^ψ must vanish at the embedded magnetic separatrix at least as fast as $\lim_{\psi_T \rightarrow \psi_T^X} \xi^\psi < o(\sqrt{|\psi_T^X - \psi_T|} \sqrt{|\ln|\psi_T^X - \psi_T||})$. But, the terms $\propto (\partial \xi^\psi / \partial \psi_T)^2$ in δW_p^i and in δW_p^c [Eq. (21)] are regularized only by an even faster vanishing,

$$\lim_{\psi_T \rightarrow \psi_T^X} \xi^\psi < o\left(\frac{\sqrt{|\psi_T^X - \psi_T|}}{\sqrt{|\ln|\psi_T^X - \psi_T||}}\right). \quad (22)$$

The terms $\propto |\vec{\nabla} \psi_T|^2 (\epsilon \partial \eta^\psi / \partial \theta + \partial \eta^\psi / \partial \phi)^2$ in δW_p^i and $\propto |\vec{\nabla} \psi_T|^2 (\eta^\psi)^2$ in δW_k [Eq. (20)], are regularized, far from the

X-point, by $\lim_{\psi_T \rightarrow \psi_T^X, |\theta - \theta_X| \sim O(1)} \eta^\psi < O(1/\sqrt{|\psi_T^X - \psi_T|} |\ln|\psi_T^X - \psi_T||)$ and, near the X-point, by $\lim_{\psi_T \rightarrow \psi_T^X, \theta \rightarrow \theta_X} \eta^\psi < O(1/\sqrt{|\psi_T^X - \psi_T|} \sqrt{|\ln|\psi_T^X - \psi_T||})$.

The terms $\propto (\mu)^2$ in δW_k , $\propto (\epsilon \partial \mu / \partial \theta + \partial \mu / \partial \phi)^2$ and $\propto (\partial \xi^\psi / \partial \psi_T) (\epsilon \partial \mu / \partial \theta + \partial \mu / \partial \phi)$ in δW_p^c are regularized by

$$\lim_{\psi_T \rightarrow \psi_T^X} \mu < O(1/\sqrt{|\psi_T^X - \psi_T|} \sqrt{|\ln|\psi_T^X - \psi_T||}).$$

Apart from the requirement of regularity for the potential and kinetic perturbed plasma energies, the physical plasma displacement $\vec{\xi}$ must be regular upon the embedded separatrix—note instead that the displacement variables η^ψ and μ are shown above to be able to diverge. The actual components of $\vec{\xi}$ are most easily expressed through the three (normal, binormal, and parallel) orthonormal vectors,

$$\vec{\xi} = \begin{bmatrix} \vec{\xi} \cdot \vec{\nabla} \psi_T \\ |\vec{\nabla} \psi_T| \end{bmatrix} \frac{\vec{\nabla} \psi_T}{|\vec{\nabla} \psi_T|} + \begin{bmatrix} \vec{\xi} \cdot (\vec{B} \wedge \vec{\nabla} \psi_T) \\ |\vec{\nabla} \psi_T| B \end{bmatrix} \frac{\vec{B} \wedge \vec{\nabla} \psi_T}{|\vec{\nabla} \psi_T| B} + \begin{bmatrix} \vec{\xi} \cdot \vec{B} \\ B \end{bmatrix} \frac{\vec{B}}{B}, \quad (23)$$

or, substituting into (6) the radial covariant basis vector⁸ $\vec{e}_\psi = \vec{\nabla} \psi_T / |\vec{\nabla} \psi_T|^2 + \beta_* \vec{B} / B^2 - \gamma_* (\vec{B} \wedge \vec{\nabla} \psi_T) / B^2$,

$$\vec{\xi} = \begin{pmatrix} \xi^\psi \\ |\vec{\nabla} \psi_T| \end{pmatrix} \frac{\vec{\nabla} \psi_T}{|\vec{\nabla} \psi_T|} + \begin{pmatrix} |\vec{\nabla} \psi_T| (\eta^\psi - \gamma_* \xi^\psi) \\ B \end{pmatrix} \frac{\vec{B} \wedge \vec{\nabla} \psi_T}{|\vec{\nabla} \psi_T| B} + \begin{pmatrix} \beta_* \xi^\psi + I \eta^\psi - \mu B^2 \\ B \end{pmatrix} \frac{\vec{B}}{B}. \quad (24)$$

The regularity condition for the normal component of $\vec{\xi}$ in (24) imposes $\lim_{\psi_T \rightarrow \psi_T^X} \xi^\psi \leq o(\sqrt{|\psi_T^X - \psi_T|} \sqrt{|\ln|\psi_T^X - \psi_T||})$,

$\lim_{\psi_T \rightarrow \psi_T^X, \theta \rightarrow \theta_X} \xi^\psi \leq O(|\ln|\psi_T^X - \psi_T||)$; both conditions are however superseded by the condition imposed upon ξ^ψ (22)

by the regularity of δW_p^i and δW_p^c : then, the normal displacement vector vanishes as

$$\lim_{\psi_T \rightarrow \psi_T^X, \theta \rightarrow \theta_X} \left| \frac{\vec{\xi} \cdot \vec{\nabla} \psi_T}{|\vec{\nabla} \psi_T|} \right| < o\left(\frac{1}{|\ln|\psi_T^X - \psi_T||}\right)$$

at the X-point and as

$$\lim_{\psi_T \rightarrow \psi_T^X, |\theta - \theta_X| \sim O(1)} \left| \frac{\vec{\xi} \cdot \vec{\nabla} \psi_T}{|\vec{\nabla} \psi_T|} \right| < o\left(\frac{\sqrt{|\psi_T^X - \psi_T|}}{|\ln|\psi_T^X - \psi_T||^{3/2}}\right)$$

far from the X-point. (26)

The only exception to the vanishing of the normal component of $\vec{\xi}$ at a magnetic separatrix with regular X-points are the $n=0$ axisymmetric modes $\vec{\xi}_{n=0}$, which can have a finite normal component,

$$\lim_{\psi_T \rightarrow \psi_T^X} \left| \frac{\vec{\xi}_{n=0} \cdot \vec{\nabla} \psi_T}{|\vec{\nabla} \psi_T|} \right| \leq O(1). \quad (27)$$

This is due to a relation (to be detailed in a forthcoming paper) that, for $n=0$ only, couples the binormal to the normal displacement variable: $(\partial \xi_{n=0}^\psi / \partial \psi_T + \partial \eta_{n=0}^\psi / \partial \theta) = \sqrt{g} \xi_{n=0}^\psi (df/d\psi_T) / R^2$; this relation simplifies the energy principle and even allows for a logarithmic divergence of the normal displacement variable $\lim_{\psi_T \rightarrow \psi_T^X, |\theta - \theta_X| \sim O(1)} \xi_{n=0}^\psi$

$\propto O(|\ln|\psi_T^X - \psi_T||)$ far from the X -point. This exception expresses the obvious fact that a “vertical instability” can displace the plasma also near a separatrix with regular X -points.

Near the X -point the regularity condition for the binormal component of $\vec{\xi}$ in (24) $\lim_{\psi_T \rightarrow \psi_T^X, \theta \rightarrow \theta_X} |\eta^\psi - \gamma_* \xi^\psi| \leq O(1/\sqrt{|\psi_T^X - \psi_T| |\ln|\psi_T^X - \psi_T||})$ is less restrictive than the condition imposed upon η^ψ by the regularity of δW_p^i and δW_k ; therefore, it does not supersede it and the binormal displacement vector vanishes at a regular X -point,

$$\lim_{\substack{\psi_T \rightarrow \psi_T^X \\ \theta \rightarrow \theta_X}} \left| \frac{\vec{\xi} \cdot \vec{\mathbf{B}} \wedge \vec{\nabla} \psi_T}{|\vec{\nabla} \psi_T| B} \right| < O(1). \quad (28)$$

The regularity condition for $\vec{\xi}$ requires instead that far from an X -point $\lim_{\psi_T \rightarrow \psi_T^X, |\theta - \theta_X| \sim O(1)} |\eta^\psi - \gamma_* \xi^\psi| \leq O(1/|\ln|\psi_T^X - \psi_T||)$, which is more restrictive than the condition imposed upon η^ψ by the regularity of δW_p^i and δW_k ; therefore, the binormal displacement vector can be finite far from the X -point,

$$\lim_{\substack{\psi_T \rightarrow \psi_T^X \\ |\theta - \theta_X| \sim O(1)}} \left| \frac{\vec{\xi} \cdot \vec{\mathbf{B}} \wedge \vec{\nabla} \psi_T}{|\vec{\nabla} \psi_T| B} \right| \leq O(1). \quad (29)$$

The asymptotic behavior of γ_* (see Sec. III) and of ξ^ψ (22) shows that $\gamma_* \xi^\psi$ always vanishes faster or diverges more slowly than η^ψ . Therefore, the asymptotic behavior of the binormal displacement variable η^ψ is restricted near the X -point by

$$\lim_{\substack{\psi_T \rightarrow \psi_T^X \\ \theta \rightarrow \theta_X}} |\eta^\psi| < O\left(\frac{1}{\sqrt{|\psi_T^X - \psi_T| |\ln|\psi_T^X - \psi_T||}}\right), \quad (30)$$

and far from it by

$$\lim_{\substack{\psi_T \rightarrow \psi_T^X \\ |\theta - \theta_X| \sim O(1)}} |\eta^\psi| \leq o\left(\frac{1}{|\ln|\psi_T^X - \psi_T||}\right). \quad (31)$$

Enforcing a regular parallel component of $\vec{\xi}$ in (24) means that

$$\lim_{\psi_T \rightarrow \psi_T^X} |\mu - \eta^\psi I / B^2 - \xi^\psi \beta_* / B^2| \leq O(1). \quad (32)$$

As the term $\beta_* \xi^\psi$ vanishes and the range (30) and (31) limits the term $I \eta^\psi$, a compensation must then exist between the

variables η^ψ and μ in the case where they diverge near the embedded magnetic separatrix; therefore,

$$\lim_{\substack{\psi_T \rightarrow \psi_T^X \\ \theta \rightarrow \theta_X}} |\mu| < O\left(\frac{1}{\sqrt{|\psi_T^X - \psi_T| |\ln|\psi_T^X - \psi_T||}}\right), \quad (33)$$

$$\lim_{\substack{\psi_T \rightarrow \psi_T^X \\ |\theta - \theta_X| \sim O(1)}} |\mu| \leq o\left(\frac{1}{|\ln|\psi_T^X - \psi_T||}\right). \quad (34)$$

The vanishing of the normal displacement variable ξ^ψ , for $n \neq 0$, matches the prescription of continuity¹³ of $\xi^\psi / |\vec{\nabla} \psi_T|$ at the embedded magnetic separatrix. The possible singularities (30) and (33) of the binormal and of the parallel displacement variables η^ψ and μ are compatible with the their permissible discontinuities¹³ at any radial position. For $n=0$ the continuity of $\xi_{n=0}^\psi / |\vec{\nabla} \psi_T|$ is still guaranteed: far from the X -point the logarithmic divergence of the variable $\xi_{n=0}^\psi \propto O(|\ln|\psi_T^X - \psi_T||)$ is exactly compensated by the divergence of $|\vec{\nabla} \psi_T| \propto |\ln|\psi_T^X - \psi_T||$.

VI. PERMISSIBLE ASYMPTOTIC LIMITS FOR THE PERTURBED DISPLACEMENT AT A SINGULAR X -POINT

At a singular X -point ($\psi_T = \psi_T^X$, $\theta = \theta_{B=0}$) the first three terms in δW_p^c [Eq. (21)] show that ξ^ψ must vanish at least faster than $\lim_{\psi_T \rightarrow \psi_T^X, \theta \rightarrow \theta_{B=0}} \xi^\psi < o(r^{3/2})$, where r is the local distance from the singular X -point. The terms $\propto (\eta^\psi)^2$, $\propto (\eta^\psi) \times (\xi^\psi)$, and $\propto (\eta^\psi)(\partial \xi^\psi / \partial \psi_T)$ in δW_p^c are regularized by the choice that η^ψ near a singular X -point vanishes faster than

$$\lim_{\psi_T \rightarrow \psi_T^{\max}, \theta \rightarrow \theta_{B=0}} \eta^\psi < o(\sqrt{r}). \quad (35)$$

The term $\propto (\mu)^2$ in δW_k [Eq. (20)] is regularized by the choice $\lim_{\psi_T \rightarrow \psi_T^{\max}, \theta \rightarrow \theta_{B=0}} \mu < O(1/r^{5/2})$. A regular normal displacement vector in (24), along with the behavior of $\vec{\nabla} \psi_T$ near a singular X -point (see Sec. III), constrains the variable ξ^ψ to vanish faster than $o(r^{3/2})$, which is what the regularity of δW_p^c would require,

$$\lim_{\psi_T \rightarrow \psi_T^{\max}, \theta \rightarrow \theta_{B=0}} |\xi^\psi| \leq o(r^2). \quad (36)$$

A regular binormal displacement vector in (24), along the behavior of $\vec{\nabla} \psi_T$ and B gives (see Sec. III) $\lim_{\psi_T \rightarrow \psi_T^{\max}, \theta \rightarrow \theta_{B=0}} |\eta^\psi - \gamma_* \xi^\psi| \leq O(1/r)$. But, as the displacement variable η^ψ vanishes at least as fast as (35) and, as from (36) and from the behavior of γ_* , $\lim_{\psi_T \rightarrow \psi_T^{\max}, \theta \rightarrow \theta_{B=0}} |\gamma_* \xi^\psi| \leq o(r)$, it means that the binormal component of $\vec{\xi}$ must vanish at a singular X -point:

$$\lim_{\psi_T \rightarrow \psi_T^{\max}, \theta \rightarrow \theta_{B=0}} |(\vec{\xi} \cdot \vec{\mathbf{B}} \wedge \vec{\nabla} \psi_T) / (|\vec{\nabla} \psi_T| B)| \leq o(r^{3/2}).$$

A regular parallel displacement vector in (24) means (as $\beta_* = 0$): $\lim_{\psi_T \rightarrow \psi_T^{\max}, \theta \rightarrow \theta_{B=0}} |\mu - \eta^\psi I / B^2| \leq O(1/r)$. Because of the

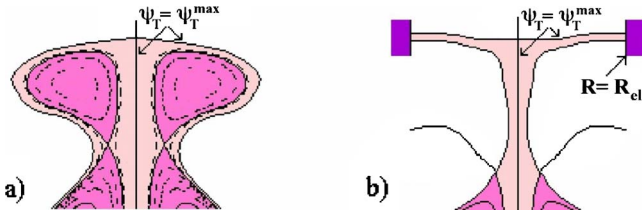


FIG. 2. (Color online) Branching of the flux surface $\psi_T = \psi_T^{\max}$ for: (a) a CKF configuration; (b) a FCS configuration.

possible divergence of the variable μ , taking into account (35) and the behavior of B (see Sec. III), a compensation must exist between the displacement variables η^ψ/B^2 and μ , in case they diverge near a singular X -point; therefore,

$$\lim_{\psi_T \rightarrow \psi_T^{\max}, \theta \rightarrow \theta_{B=0}} |\mu| \leq O\left(\frac{1}{r^{3/2}}\right). \quad (37)$$

VII. CHANGE OF VARIABLES FOR PLASMA EXTENDING UP TO THE SYMMETRY AXIS

The perturbed displacement $\vec{\xi}$ has been expressed up to now, as in (6)–(9), in terms of the normal ξ^ψ , binormal η^ψ , and parallel μ displacement variables. However, this choice is not the best one if the plasma extends until the symmetry axis, $\psi_T^{\text{edge}} = \psi_T^{\max}$, $R=0$. As a matter of fact, for $R \rightarrow 0$, $\vec{\nabla} \psi_T \rightarrow 0$ as $|\vec{\nabla} \psi_T| \propto R$; therefore, the condition $\xi^\psi(\psi_T^{\max})=0$ should be imposed in the stability solution. Nevertheless, on top and bottom of both CKF and FCS configurations, after the singular X -point, the flux surface $\psi_T^{\text{edge}} = \psi_T^{\max}$ does not coincide anymore with the symmetry axis (Fig. 2); therefore, the condition $\xi^\psi(\psi_T^{\max})=0$ cannot be imposed in a free-boundary [i.e., $\vec{\xi}(\psi_T^{\text{edge}}) \neq 0$] ideal MHD stability calculation.

The perturbed normal displacement can be derived from the perturbed vector potential, $\vec{\nabla}^2 \vec{A} = \mu_0 \vec{j}$. Near the magnetic axis ($R=0$) the regular multipolar terms (solutions of the vector Laplace equation) give¹⁵ $|\vec{B}| \propto |\vec{\nabla} \wedge \vec{A}| \propto R^{n-1}$; therefore, the asymptotic behavior is $\xi^\psi \propto R^n$. A change of variable for the normal displacement $\xi^\psi = \xi R^N$ (with $N \geq 1$) is able to decouple the symmetry axis ($R=0$) from the plasma edge, which are both described by $\psi_T = \psi_T^{\max}$. Also, at a singular X -point on the symmetry axis the prescription that

$\lim_{\psi_T \rightarrow \psi_T^{\max}, \theta \rightarrow \theta_{B=0}} \eta^\psi < o(\sqrt{r})$ must hold (see Sec. VI). So, a regu-

larity condition $\eta^\psi(\psi_T^{\max})=0$ should be imposed in the stability solution, but it cannot be, as no radial derivative of the binormal displacement $\partial \eta^\psi / \partial \psi_T$ appears in the energy principle: the change of the binormal displacement variable $\eta^\psi = \eta B$ removes the need for any regularity condition at a singular X -point. In terms of the new displacement variables (ξ , η , μ) the physical perturbed plasma displacement becomes

$$\begin{aligned} \vec{\xi} = & \xi R^N \frac{\vec{\nabla} \psi_T}{|\vec{\nabla} \psi_T|^2} + \left(\eta - \gamma_* \frac{R^N}{B} \xi \right) \frac{\vec{B} \wedge \vec{\nabla} \psi_T}{B} \\ & + \left(\beta_* \frac{R^N}{B^2} \xi + \frac{I}{B} \eta - \mu \right) \vec{B}. \end{aligned} \quad (38)$$

The choice of the exponent N to be used in the normal displacement variable, $\xi^\psi = \xi R^N$, is determined requiring that the incompressible plasma magnetic energy does not diverge near the symmetry axis ($R=0$). The first term in δW_p^i [Eq. (14)] is the one most at risk of divergence: $1/2 \mu_0 \int_0^{\psi_T^{\max}} d\psi_T \int_0^{2\pi} d\phi \int_{\theta_{\min}}^{\theta_{\max}} d\theta \{ \dots \sqrt{g} B^2 N^2 R^{2N-2} (\partial R / \partial \psi_T)^2 (\xi)^2 \dots \}$. This integral near $R=0$ becomes $\delta W_p^i \propto \int_0^R dR \{ \dots R R^{2N-2} (1/R)^2 (\xi)^2 \dots \}$; therefore, the smallest integer exponent which avoids divergences is $N=2$.

Making this change of variables and using the Fourier expansion, this time for ξ and η , the incompressible perturbed potential plasma energy is again expressed as a quadratic form in the variables ξ_ℓ and η_ℓ and in the radial derivative of the normal variable $\partial \xi_\ell / \partial \psi_T$; the perturbed compressible kinetic energy is also expressed as a quadratic form in the variables $(\xi_\ell, \eta_\ell, \mu_\ell)$, and the compressible potential plasma energy is finally expressed as a quadratic form in the variables ξ_ℓ and η_ℓ and in the derivatives $\partial \xi_\ell / \partial \psi_T$, $\partial \eta_\ell / \partial \theta$ and $\epsilon \partial \mu_\ell / \partial \theta + \partial \mu_\ell / \partial \phi$. Modified poloidal contour integrals $\tilde{C}_{\ell\ell}^{(i)}(\psi_T)$ (with $i=0, 1, \dots, 39$), $\tilde{K}_{\ell\ell}^{(i)}(\psi_T)$ (with $i=0, 1, \dots, 7$) and $\tilde{D}_{\ell\ell}^{(i)}(\psi_T)$ (with $i=0, 1, \dots, 14$)—not written in this paper—must be introduced.

VIII. INTEGRATION OF VACUUM PERTURBED ENERGY

In the calculation of the ideal MHD stability, the numerical normal-mode equation

$$\vec{W} \cdot |\vec{x}\rangle = \omega^2 \vec{K} \cdot |\vec{x}\rangle \quad (39)$$

must be radially discretized over the mesh points ψ_T^j , $j=0, 1, \dots, N_\psi$ and solved, finding the eigenfunction $|\vec{x}\rangle \equiv (\xi_\ell^j, \eta_\ell^j, \mu_\ell^j)$ with the minimum eigenvalue ω^2 ; the numerically discretized potential energy matrix \vec{W} and the kinetic energy matrix \vec{K} (positive definite) are symmetric and block diagonal. The radial behavior of $\xi_\ell(\psi_T)$, $\eta_\ell(\psi_T)$, $\mu_\ell(\psi_T)$, and $\partial \xi_\ell / \partial \psi_T$ is approximated by a one-dimensional finite-element method.¹³ For $\xi_\ell(\psi_T)$ the hat functions $\mathbf{e}_j(\psi_T)$, $j=0, 1, \dots, N_\psi$ are used. For $\eta_\ell(\psi_T)$, $\mu_\ell(\psi_T)$, and $\partial \xi_\ell / \partial \psi_T$ the piecewise constant functions $\mathbf{c}_{j-1/2}(\psi_T)$, $j=1, 2, \dots, N_\psi$ are used. The finite hybrid element representation is then $\xi_\ell^j \equiv \xi_\ell(\psi_T^j)$, $\eta_\ell^j \equiv \eta_\ell(\psi_T^{j-1/2})$, $\mu_\ell^j \equiv \mu_\ell(\psi_T^{j-1/2})$, and $\partial \xi_\ell^j / \partial \psi_T = (\xi_\ell^j - \xi_\ell^{j-1}) / (\psi_\ell^j - \psi_\ell^{j-1})$. As the first mesh point ($j=0$) is calculated at the magnetic axis $\psi_T=0$, the regularity condition $\xi_\ell^0=0$ could well be imposed; as a matter of fact this condition can be avoided in the STABLE code, as the behavior of the poloidal contour integrals $C_{\ell\ell}^{(i)}(\psi_T)$, $K_{\ell\ell}^{(i)}(\psi_T)$, and $D_{\ell\ell}^{(i)}(\psi_T) \times (\psi_T)$ constrains $\xi_\ell^0(0) \rightarrow 0$. The simplest boundary condition at the edge of the plasma is the fixed-boundary condition $\xi^\psi(\psi_T^{\text{edge}})=0$, which can be directly enforced into (39) and corresponds to a perfectly conducting shell in contact with the plasma boundary. More interesting is the free-boundary

condition, where the (eventual) conducting shells are placed at a distance from the plasma edge, which is therefore free to move, i.e., $\xi^\psi(\psi_T^{\text{edge}}) \neq 0$. The normal-mode equation is modified by the free-boundary vacuum magnetic energy through an additional term¹⁶ present only upon the last ($j=N_\psi$) radial mesh point $\psi_T^{N_\psi}$,

$$\delta W_p(\vec{\xi}^*, \vec{\xi}) + \delta W_v[\xi^{\psi*}(\psi_T^{N_\psi}), \xi^\psi(\psi_T^{N_\psi})] = \omega^2 \delta W_k(\vec{\xi}^*, \vec{\xi}). \quad (40)$$

The integration of the vacuum perturbed energy is sketched in this paper only for the plasma configurations composed by closed flux surfaces, respectively, for doubly connected axisymmetric toroidal plasmas (tokamaks) and for simply connected configurations like CKF; the discussion of the magnetic configurations composed in part by open flux surfaces will be deferred to a forthcoming paper. The perturbed vacuum energy can be derived¹⁶ from the vacuum solution to the perturbed field, expressed through the two-dimensional magnetic scalar potential in cylindrical coordinates (R, φ, Z) ,

$$\Phi = \tilde{\Phi}^c \cos(n\varphi) + \tilde{\Phi}^s \sin(n\varphi). \quad (41)$$

Introducing, only upon the poloidal contour l_ψ of the plasma cross section, the quantities \tilde{B}^{nc} and \tilde{B}^{ns} ,

$$\tilde{B}^{nc} = \mu_0 \sqrt{g} |\vec{\nabla} \psi_T| (\partial \tilde{\Phi}^{nc} / \partial n) |_{\psi_T^{N_\psi}}; \quad (42)$$

$$\tilde{B}^{ns} = \mu_0 \sqrt{g} |\vec{\nabla} \psi_T| (\partial \tilde{\Phi}^{ns} / \partial n) |_{\psi_T^{N_\psi}},$$

where $(\partial / \partial n)$ means the normal derivative at the plasma surface; the vacuum perturbed energy becomes a contour integral over the poloidal Boozer angle,

$$\delta W_v = \frac{\pi}{2} \oint_{\ell_\psi} [\tilde{\Phi}^{nc} \tilde{B}^{nc} + \tilde{\Phi}^{ns} \tilde{B}^{ns}] d\theta. \quad (43)$$

In the vacuum region between the plasma surface and the perfectly conducting shells, the Laplace equation obeyed by $\tilde{\Phi}^{nc}$ and $\tilde{\Phi}^{ns}$,

$$\frac{1}{R} \frac{\partial}{\partial R} \left(R \frac{\partial \tilde{\Phi}^{nc/s}}{\partial R} \right) + \frac{\partial^2 \tilde{\Phi}^{nc/s}}{\partial Z^2} - \frac{n^2}{R^2} \tilde{\Phi}^{nc/s} = 0, \quad (44)$$

is solved by a 2D finite-element method. The boundary condition for the plasma edge surface S_ψ is $\mu_0 \vec{\nabla} \Phi |_{\psi_T^{N_\psi}} \cdot d\vec{S}_\psi = -\vec{\nabla} \wedge (\vec{\xi} \wedge \vec{B}) |_{\psi_T^{N_\psi}} \cdot d\vec{S}_\psi$, which gives

$$\partial \Phi / \partial n |_{S_\psi} = (\epsilon \partial \xi^\psi / \partial \theta + \partial \xi^\psi / \partial \phi) / (\mu_0 \sqrt{g} |\vec{\nabla} \psi_T|) |_{\psi_T^{N_\psi}} \quad (45)$$

and the boundary conditions on the axisymmetric ideal conducting shells S_c (which can either surround or not surround the plasma) is $\vec{\nabla} \Phi \cdot d\vec{S}_c = 0$, which gives

$$\partial \Phi / \partial n |_{S_c} = 0. \quad (46)$$

Both surface elements $d\vec{S}_\psi$ and $d\vec{S}_c$ are oriented out from the vacuum region.

In the case of a tokamak not limited by a magnetic separatrix, the last radial mesh point coincides with the plasma

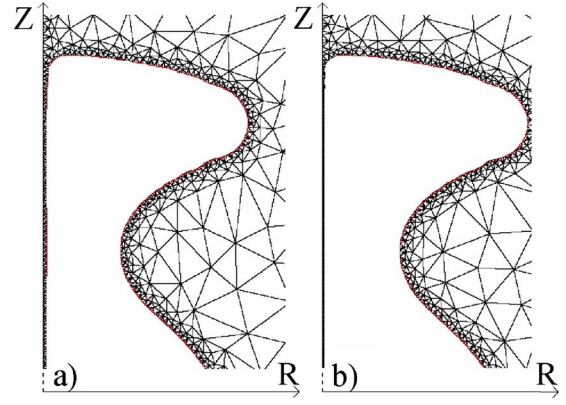


FIG. 3. (Color online) Details of vacuum 2D finite element mesh for CKF configuration: (a) last plasma surface farther from $R=0$ and vacuum region surrounding the symmetry axis; (b) last plasma surface nearer to $R=0$ and infinitesimally thin conductor on the symmetry axis.

edge: $\psi_T^{N_\psi} = \psi_T^{\text{edge}}$. If there is a magnetic separatrix at the edge of the plasma, an intensified numerical radial mesh is set up: the various divergences, summarized in Sec. III, compel to stop the calculation of the Boozer coordinates and of the perturbed energy before the minimum distances from the magnetic separatrix where $\epsilon(\psi)$ can still be calculated numerically (typically at $\psi_T^{N_\psi} = \psi_T^X - \epsilon_{ST} / 2\pi \epsilon_X$, with $\epsilon_{ST} \approx (10^{-3} - 10^{-2}) |\psi_{\text{max}} - \psi_X|$ and $\epsilon_X = \epsilon(\psi_T^{N_\psi})$, where ψ_{max} is the poloidal flux at the magnetic axis.

The calculation of the ideal MHD stability of a simply connected plasma—extending until the symmetry axis (i.e., $R=0$, $\psi_T = \psi_T^{\text{max}}$)—deals, in free-boundary condition [i.e., $\vec{\xi}(\psi_T^{\text{max}}, \theta, \phi) \neq 0$], with a simply connected conducting shell, which can be at finite or infinite distance from the plasma edge. Nevertheless, in the numerical code (see Fig. 3)

- either the last mesh point with $j=N_\psi$ is located at $\psi_T = \psi_T^{\text{max}} - \epsilon_{\text{symm}} / 2\pi \epsilon_{\text{symm}}$ and a vacuum region replaces the plasma in the very small region around the symmetry axis; or
- a doubly connected conducting shell, closed on the symmetry axis by an infinitesimally thin conductor, replaces the simply connected conducting shell.

The effect upon the stability threshold of the two different assumptions is only marginal, as will be illustrated in a forthcoming paper, along with the 2D finite-element method used for solving the Laplace equation in the vacuum region.

IX. NUMERICAL RESULTS NEAR THE EMBEDDED MAGNETIC SEPARATRIX

In general, at an edge magnetic separatrix (irrespective of whether it has regular or singular X -points) it can be shown that the radial derivatives of the perturbed potential plasma energy δW_p (3) and of the free-boundary vacuum perturbed magnetic energy δW_v (43) are opposite:

$$\lim_{\psi_T^{N_\psi} \rightarrow \psi_T^X} [\partial(\delta W_v + \delta W_p) / \partial \psi_T] |_{\psi_T^{N_\psi}} = 0, \text{ if no surface equilibrium}$$

plasma current flows at the plasma-vacuum boundary. So, near the edge separatrix the choice of the last magnetic sur-

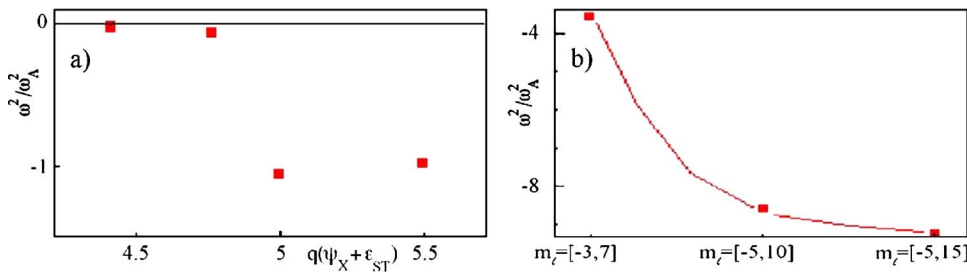


FIG. 4. (Color online) (a) Behavior of ω^2/ω_A^2 , for a FCS configuration unstable to $n=1$, as a function of the radial distance of the last ST radial mesh point ($\psi = \psi_X + \varepsilon_{ST}$) from the embedded magnetic separatrix ($\psi = \psi_X$). The distance ε_{ST} is expressed through the value of the safety factor $q(\psi_X + \varepsilon_{ST})$. (b) Behavior of ω^2/ω_A^2 , for a different FCS example, as a function of the spectrum of poloidal mode numbers.

face ($j=N_\psi$) for the stability calculation does not seem particularly critical, as the dominant errors in the plasma and in the vacuum magnetic energies compensate exactly.

Much more critical is the choice of the intensified numerical radial mesh near an embedded magnetic separatrix, which must be refined enough as to match *a posteriori* the permissible asymptotic limits for ξ . When plasma is present on both sides of the embedded separatrix, the field lines, labeled by $\theta_0 = \theta - \varepsilon(\psi)\phi$, must be in correspondence at the ST-SP interface. The continuity of the normal variable ξ^ψ implies the continuity of the angles θ and ϕ and forces the matching condition,

$$\varepsilon^{SP}(\psi_X - \varepsilon_{SP}) = \varepsilon^{ST}(\psi_X + \varepsilon_{ST}) = \varepsilon_X \quad (47)$$

between the two adjacent radial mesh points on the two sides of the separatrix. In any MHD axisymmetric equilibria, in terms of the poloidal flux ψ , the rotational transform near the separatrix exhibits the logarithmic behavior,⁸

$$\lim_{\psi \rightarrow \psi_X} \varepsilon(\psi) = -A/\ln|C(\psi - \psi_X)|. \quad (48)$$

A characteristic of FCS configurations [see Fig. 1(b)] is that the rotational transform calculated on the ST side is about the same as the rotational transform, calculated at the same distance on the SP side: $\varepsilon_{FCS}^{SP}(\psi_X - \varepsilon) \approx \varepsilon_{FCS}^{ST}(\psi_X + \varepsilon)$; this allows for simple solutions of the matching condition (47), where ε_{ST} is always of the same order⁸ of ε_{SP} . Typical minimum distances of the last mesh point from the embedded separatrix are $\varepsilon_{ST} \approx (10^{-3} - 5 \times 10^{-3})|\psi_{\max} - \psi_X|$; typical corresponding values of the rotational transform are $2\pi\varepsilon_X^{ST} \approx 2\pi\varepsilon_X^{SP} \approx 0.5 - 1$. Figure 4(a) shows the effect of the distance between the radial mesh and the separatrix upon the most unstable eigenvalue calculated by the numerical code; the results are expressed as the ratio between the square of the growth rate of the instability ω^2 and the squared Alfvén rate $\omega_A^2 = B_0^2/\mu_0\rho_0R_0^2$, where R_0 is the magnetic axis, upon which the toroidal field strength is B_0 and the plasma density is ρ_0 (assumed constant all over the plasma). The radial distance ε_{ST} between the radial mesh and the separatrix has been decreased, in the FCS example of Fig. 4(a), from $\varepsilon_{ST} = 2 \times 10^{-2}|\psi_{\max} - \psi_X|$ (which corresponds to a safety factor $q_X = 1/\varepsilon_X = 4.4$) down to $\varepsilon_{ST} = 2 \times 10^{-3}|\psi_{\max} - \psi_X|$ (which corresponds to a safety factor $q_X = 1/\varepsilon_X = 5.5$). It is a general result that, for both FCS as well as for CKF configurations, acceptable convergence of the most unstable eigenvalue is obtained only if $\varepsilon_{ST} < 1 \times 10^{-2}|\psi_{\max} - \psi_X|$, which typically corresponds to a distance $|\psi_T^X - \psi_T| < 2.5 \times 10^{-2}\psi_T^X$, when expressed in terms of the radial Boozer coordinate ψ_T . The study of con-

vergence of the most unstable eigenvalue as a function of the broadness of the spectrum of poloidal mode numbers is illustrated in Fig. 4(b), for a different FCS example. The choice of $m_\ell = [-5, 15]$ for the poloidal spectrum represents a reasonable convergence.

For CKF configurations [see Fig. 1(a)], the rotational transform on the ST side is instead calculated to be about twice as much as the rotational transform calculated at the same distance on the SP side (see Fig. 5): $\varepsilon_{CKF}^{ST}(\psi_X + \varepsilon) \approx 2\varepsilon_{CKF}^{SP}(\psi_X - \varepsilon)$; therefore, given $\varepsilon_{SP} \approx (4 \times 10^{-3} - 2 \times 10^{-2})|\psi_{\max} - \psi_X|$, the matching condition (47) is used to find ε_{ST} —fitting the logarithmic behavior (48) and extrapolating it on the ST side to much smaller values, typically $\varepsilon_{ST} \sim 10^{-5}\varepsilon_{SP}$. The values found for $|\ln C|$ at the minimum distance ε_{SP} still amount to 17–40% of $\ln|\psi - \psi_X|$, implying that numerical errors in forcing the matching condition (47) are unavoidable.

The radial mesh of a numerical run for a CKF configuration is typically composed by 140 radial points: 70 inside the ST—30 of which are concentrated near the separatrix, 40 inside the SP—20 of which are concentrated near the separatrix and 30 in either of the two up/down symmetric SCs. The numerical results are compared *a posteriori* with the permissible asymptotic limits for the perturbed displacement. In this paper the behavior of the unstable eigenfunctions will only be presented inside the ST plasma of the magnetic configurations; the couplings between the ST, the SP, and the SC plasmas, have only the effect of increasing the bandwidth of the numerical normal-mode equation, as will be discussed in a forthcoming paper. Figure 6 shows the numerical perturbed displacement arrow plot in the poloidal plane, for three CKF configurations, respectively, unstable to $n=3$ [Fig. 6(a)] and to $n=1$ toroidal mode numbers [Figs. 6(b) and 6(c)]; in all three cases the instability is limited inside the ST plasma and the numerically accounted couplings with the SP and the SC plasmas are not effective. Figure 6 confirms that

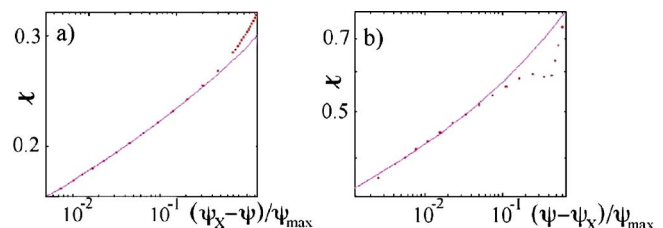


FIG. 5. (Color online) Fit (line) to numerical rotational transform (dots) near the embedded magnetic separatrix, for the CKF configuration of Fig. 1(a): (a) on the SP side; (b) on the ST side.

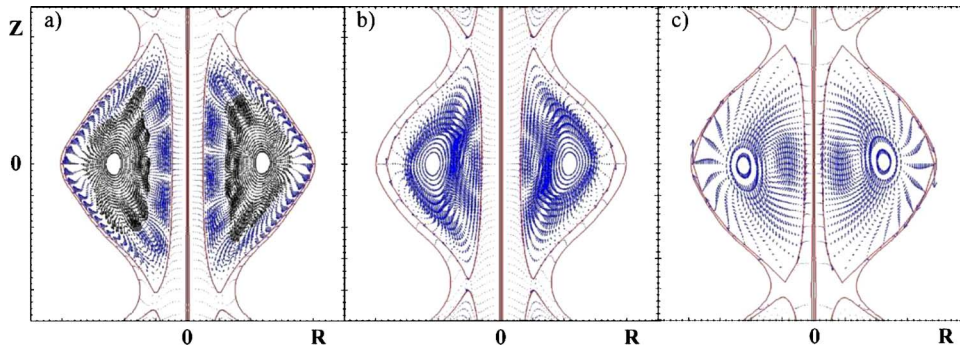


FIG. 6. (Color online) Poloidal cross section of the perturbed displacement arrow plot for CKF configurations. (a) CKF with volume averaged $\langle\beta\rangle_{ST}=2\mu_0\langle p\rangle_{ST}/\langle B^2\rangle_{ST}=1$, currents ratio $I_{ST}/I_e=6.5$, and safety factor on axis $q_0^{ST}=1.11$, unstable to $n=3$; the main mode is $m/n=5/3$; the arrows near the ST magnetic axis have been enlarged and reveal a subdominant structure $m/n=4/3$. (b) CKF with $\langle\beta\rangle_{ST}=0$, $I_{ST}/I_e=2$, $q_0^{ST}=1.72$, unstable to $n=1$; the main mode is $m/n=2/1$ with a subdominant structure $m/n=4/1$. (c) CKF with $\langle\beta\rangle_{ST}=0$, $I_{ST}/I_e=14.4$, $q_0^{ST}=1.08$, unstable to $n=1$; the main mode is $m/n=1/1$, with a subdominant structure $m/n=2/1$.

- The normal perturbed displacement vanishes (25) near the X-point and far from it (26).
- The binormal perturbed displacement vanishes (28) near the X-point, but is finite far from it (29).
- Although not visible from the poloidal plane arrow plots of Fig. 6, the parallel perturbed displacement (32) is finite along the whole embedded magnetic separatrix.

The results for the main Fourier components ($m_\ell=0, 1,$ and 2) of the numerical displacement variables $|\vec{x}\rangle \equiv (\xi_\ell^j, \eta_\ell^j, \mu_\ell^j)$ are shown in Fig. 7 on the ST side of the embedded separatrix, for the CKF configuration of Fig. 6(c), unstable to $n=1$. The vanishing of the computational normal variables ξ_ℓ^j ($j=0, 1, \dots, N_\psi$; see Fig. 7) is always quite near its most unstable vanishing asymptotic limit (22): $\lim_{\psi_T \rightarrow \psi_T^X} \xi_\ell^j(\psi_T) \sim o(\sqrt{|\psi_T^X - \psi_T|} / \sqrt{|\ln|\psi_T^X - \psi_T||})$. Near the embedded separatrix the numerical binormal and parallel variables, η_ℓ^j and μ_ℓ^j (with $j=1, 2, \dots, N_\psi$) can span all their asymptotic permissible ranges (30–31 and 33–34) and the variable μ_ℓ^j , if diverging, compensates (32) the divergence of η_ℓ^j . In particular: for the case of Fig. 6(a) the asymptotic numerical behaviors are $\lim_{\psi_T \rightarrow \psi_T^X} [|\eta^\psi(\psi_T)|, |\mu(\psi_T)|] \sim o(1/|\ln|\psi_T^X - \psi_T||)$, i.e. they vanish radially approaching the embedded separatrix; for the case of Fig. 6(b) $\lim_{\psi_T \rightarrow \psi_T^X} (|\eta^\psi(\psi_T)|, |\mu(\psi_T)|) \sim O(1)$, i.e., they are radially constant approaching the regular X-point; for the case

of Fig. 6(c) $\lim_{\psi_T \rightarrow \psi_T^X} [|\eta^\psi(\psi_T)|, |\mu(\psi_T)|] \sim O[1/(\sqrt{|\psi_T^X - \psi_T|} |\ln|\psi_T^X - \psi_T||^{3/2})]$, i.e., they diverge radially approaching the regular X-point (see Fig. 7).

Near an embedded separatrix the STABLE code, due to the not so large values of $q_X=1/\iota_X \leq 5-6$ at which the rotational transform can still be calculated numerically, is at present not able to deal with high $q=m_\ell/n$ modes localized at the separatrix: first, many relevant quantities at any point with $q > q_X$ would indeed be computed just by extrapolations; second, increasing the limit of the poloidal spectrum much beyond $m_\ell = [-5, 15]$ would produce unacceptably long computational times and third, the present refined mesh has fixed steps of about $|\psi_T^j - \psi_T^{j-1}| \sim 7 \times 10^{-3} \psi_T^X$, meaning that typically only 2–3 mesh points are present in the region $4 < q < 5$ near the separatrix. Therefore, the limit for modes resonating on the separatrix is $q=m_\ell/n \leq 6$ for $n=1$, $q=m_\ell/n < 4$ for $n=2$, and $q=m_\ell/n < 3$ for $n=3$. As a matter of fact, a subdominant mode with $m_\ell/n=7/3$ can be spotted at the edge in Fig. 6(a) and an edge mode with $m_\ell/n=8/3$ is more clearly observed in Fig. 8, indicating that an adaptive refinement of both the mesh size as well as of the broadness of the poloidal spectrum should be able to deal with more localized unstable modes.

The behavior of the numerical displacement variables $|\vec{x}\rangle \equiv (\xi_\ell^j, \eta_\ell^j, \mu_\ell^j)$ near the singular X-points of the edge mag-

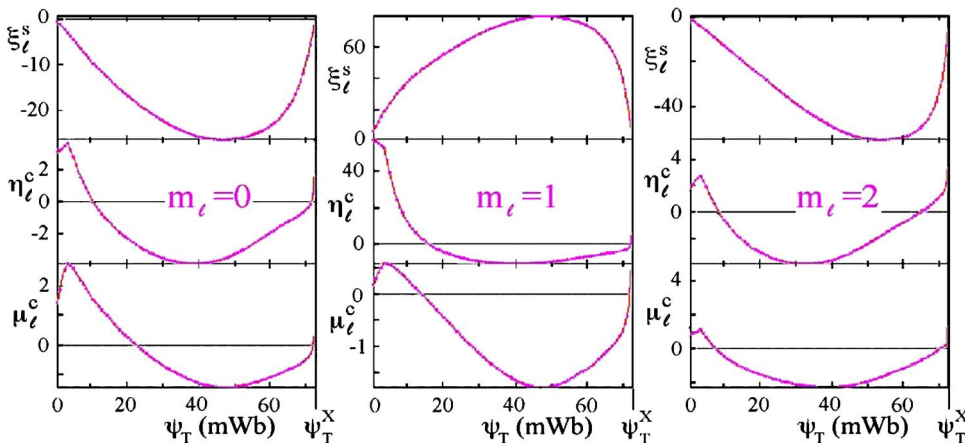


FIG. 7. (Color online) Fourier components of the perturbed displacement variables $(\xi_\ell^j, \eta_\ell^j, \mu_\ell^j)$ with $m_\ell=0, 1, 2$ inside the ST for an $n=1$ unstable mode of the CKF configuration shown in Fig. 6(c).

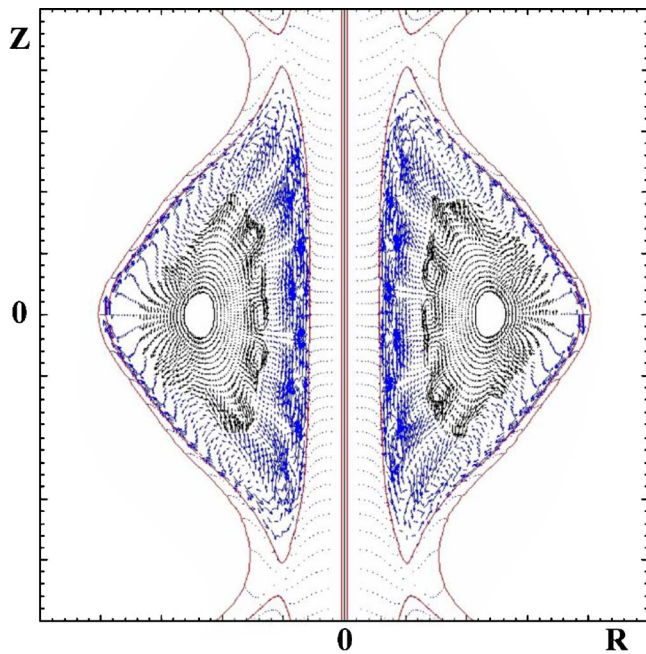


FIG. 8. (Color online) Poloidal cross section of the perturbed displacement arrow plot. (a) CKF configuration with volume averaged $\langle \beta \rangle_{ST} = 2\mu_0 \langle p \rangle_{ST} / \langle B^2 \rangle_{ST} = 1$, $I_{ST}/I_e = 4.0$, and $q_0^{ST} = 1.32$, unstable to $n=3$; the main mode is $m/n=6/3$; the arrows near the ST magnetic axis have been enlarged and reveal a subdominant structure $m/n=5/3$; a further subdominant mode at the edge of the ST is $m/n=8/3$.

netic separatrix will not be examined in this paper, but is in good agreement with the analytical results (35)–(37).

X. SUMMARY

Taking into account all the sources of divergence connected with the asymptotic behavior of $\vec{\nabla}\psi_T$, $\vec{\nabla}\theta$, \mathbf{t} , γ_* , $d\mathbf{t}/d\psi_T$, of the metric coefficients $g_{ij} = \vec{\mathbf{e}}_i \cdot \vec{\mathbf{e}}_j$ and of some among their radial and poloidal derivatives, the permissible asymptotic limits for the perturbed displacement variables $(\xi^\psi, \eta^\psi, \mu)$ and for the vector components of $\vec{\xi}$ (normal $[\vec{\xi} \cdot \vec{\nabla}\psi_T / |\vec{\nabla}\psi_T|]$, binormal $[\vec{\xi} \cdot (\vec{\mathbf{B}} \wedge \vec{\nabla}\psi_T) / |B\vec{\nabla}\psi_T|]$, and parallel $[\vec{\xi} \cdot \vec{\mathbf{B}}/B]$), can be calculated analytically at both separatrices, imposing

- (1) The regularity of all plasma perturbed energies $\delta W_p(\vec{\xi}^*, \vec{\xi})$ and $\delta W_k(\vec{\xi}^*, \vec{\xi})$;
- (2) The regularity of the perturbed displacement $\vec{\xi}$.

At the embedded magnetic separatrix ($\psi_T = \psi_T^X$) the asymptotic limits for the displacement variables are, for $n \neq 0$,

$$\lim_{\psi_T \rightarrow \psi_T^X} \xi^\psi < o(\sqrt{|\psi_T^X - \psi_T|} \sqrt{|\ln|\psi_T^X - \psi_T||})$$

all along the magnetic separatrix,

$$\lim_{\psi_T \rightarrow \psi_T^X, \theta \rightarrow \theta_X} (|\eta^\psi|, |\mu|) < O(1/\sqrt{|\psi_T^X - \psi_T|} \sqrt{|\ln|\psi_T^X - \psi_T||})$$

near the X-point, and

$$\lim_{\psi_T \rightarrow \psi_T^X, |\theta - \theta_X| \sim O(1)} (|\eta^\psi|, |\mu|) \leq o(1/|\ln|\psi_T^X - \psi_T||)$$

far from it.

For $n=0$ there is a slower vanishing of the normal displacement variable near the X-point,

$$\lim_{\psi_T \rightarrow \psi_T^X, \theta \rightarrow \theta_X} \xi_{n=0}^\psi \leq o(\sqrt{|\psi_T^X - \psi_T|} \sqrt{|\ln|\psi_T^X - \psi_T||})$$

and a logarithmic divergence

$$\lim_{\psi_T \rightarrow \psi_T^X, |\theta - \theta_X| \sim O(1)} \xi_{n=0}^\psi \leq O(|\ln|\psi_T^X - \psi_T||)$$

far from it.

The normal component of $\vec{\xi}$ at a separatrix with regular X-points can be finite for the axisymmetric modes ($n=0$), but vanishes for all other toroidal mode numbers ($n \neq 0$). For any toroidal mode number the binormal component can be finite far from the X-point, while vanishing at the X-point, and the parallel component of $\vec{\xi}$ can be finite along the whole magnetic separatrix.

At the edge magnetic separatrix, near a singular X-point ($\psi_T = \psi_T^{\max}$, $\theta = \theta_{B=0}$, $r=0$), the results for the displacement variables are

$$\lim_{\psi_T \rightarrow \psi_T^{\max}, \theta \rightarrow \theta_{B=0}} |\xi^\psi| \leq o(r^2);$$

$$\lim_{\psi_T \rightarrow \psi_T^{\max}, \theta \rightarrow \theta_{B=0}} |\eta^\psi| < o(\sqrt{r});$$

$$\lim_{\psi_T \rightarrow \psi_T^{\max}, \theta \rightarrow \theta_{B=0}} |\mu| \leq O(1/r^{3/2});$$

but, in case of divergence, the parallel and the binormal displacement variables compensate each other,

$$\lim_{\psi_T \rightarrow \psi_T^{\max}, \theta \rightarrow \theta_{B=0}} |\mu - \eta^\psi / B^2| \leq O(1/r).$$

As far as the results of the STABLE code, the numerical unstable eigenvectors $|\vec{\mathbf{x}}\rangle \equiv (\xi_\ell^i, \eta_\ell^i, \mu_\ell^i)$ are in good agreement with the permissible asymptotic limits for $\vec{\xi}$, within the ranges of distance $|\psi_T^X - \psi_T| \leq 2.5 \times 10^{-2} \psi_T^X$ and $|\psi_T^{\max} - \psi_T| \leq 2.5 \times 10^{-2} |\psi_T^{\max} - \psi_T^X|$, respectively, from either of the two magnetic separatrices, under the conditions that at least all poloidal numbers in the interval $m_\ell = [-5, 15]$ are used and that the minimum distances between the radial mesh and either of the two separatrices are at least $|\psi_T^X - \psi_T| \leq (3-9) \times 10^{-3} \psi_T^X$ and $|\psi_T^{\max} - \psi_T| \leq (3-9) \times 10^{-3} |\psi_T^{\max} - \psi_T^X|$, respectively. The present version of the STABLE code, however, misses adaptable radial mesh size and adaptable poloidal spectrum broadness and is therefore limited to the analysis of low toroidal and poloidal mode numbers: $m_\ell/n \leq 6$ for $n=1$, $m_\ell/n < 4$ for $n=2$, and $m_\ell/n < 3$ for $n=3$.

While the radial numerical displacement variable ξ^ψ is found to be always near its most unstable asymptotic limit at both magnetic separatrices, the full range of permissible asymptotic behaviors can be obtained for the numerical

binormal and parallel displacement variables η^ψ and μ . This conclusion agrees with the dominant role that the radial dis-

placement variable plays in the stability calculation for global ideal MHD instabilities.

APPENDIX A: 1D INCOMPRESSIBLE POTENTIAL PLASMA ENERGY

After the Fourier expansion (17)–(19) and integrating over θ , Eq. (14) becomes

$$\begin{aligned}
 \left(\frac{2}{4\pi^2}\delta W_p^i\right) = & \frac{1}{2\mu_0} \int_0^{\psi_T^{\text{edge}}} d\psi_T \sum_{\ell, \ell'} \left\{ \left(\frac{\partial \xi_\ell}{\partial \psi_T}\right) [(f + \epsilon I) C_{\ell, \ell'}^{(0)}(\psi_T)] \left(\frac{\partial \xi_{\ell'}}{\partial \psi_T}\right) + \left(\frac{\partial \xi_{\ell'}}{\partial \psi_T}\right) \left[I \left(\frac{d\epsilon}{d\psi_T}\right) C_{\ell, \ell'}^{(0)}(\psi_T) - (\epsilon m_{\ell'} - n) C_{\ell, \ell'}^{(1)}(\psi_T) \right. \right. \\
 & + \left. \left(\mu_0 \frac{dp}{d\psi_T}\right) C_{\ell, \ell'}^{(2)}(\psi_T) \right] (\xi_{\ell'}) + (\xi_\ell) \left[I \left(\frac{d\epsilon}{d\psi_T}\right) C_{\ell, \ell'}^{(0)}(\psi_T) + (\epsilon m_\ell - n) C_{\ell, \ell'}^{(1)}(\psi_T) + \left(\mu_0 \frac{dp}{d\psi_T}\right) C_{\ell, \ell'}^{(2)}(\psi_T) \right] \left(\frac{\partial \xi_\ell}{\partial \psi_T}\right) + (\xi_\ell) \\
 & \times \left[\frac{I^2}{(f + \epsilon I)} \left(\frac{d\epsilon}{d\psi_T}\right)^2 C_{\ell, \ell'}^{(0)}(\psi_T) + \mu_0 \frac{I}{(f + \epsilon I)} \left(\frac{dp}{d\psi_T}\right) \left(\frac{d\epsilon}{d\psi_T}\right) C_{\ell, \ell'}^{(2)}(\psi_T) + (\epsilon m_\ell - n)(\epsilon m_{\ell'} - n) C_{\ell, \ell'}^{(3)}(\psi_T) - \left(\frac{d\epsilon}{d\psi_T}\right) \right. \\
 & \times \{ (\epsilon m_{\ell'} - n) - (\epsilon m_\ell - n) \} C_{\ell, \ell'}^{(4)}(\psi_T) - \left(\frac{d\epsilon}{d\psi_T}\right) C_{\ell, \ell'}^{(5)}(\psi_T) + \frac{1}{(f + \epsilon I)} \left(\frac{d\epsilon}{d\psi_T}\right)^2 C_{\ell, \ell'}^{(6)}(\psi_T) + \left(\mu_0 \frac{dp}{d\psi_T}\right) C_{\ell, \ell'}^{(7)}(\psi_T) \left. \right] (\xi_{\ell'}) \\
 & + \left(\frac{\partial \xi_\ell}{\partial \psi_T}\right) \left[- (fm_{\ell'} + In) C_{\ell, \ell'}^{(0)}(\psi_T) \right] (\eta_{\ell'}) + (\eta_\ell) \left[- (fm_\ell + In) C_{\ell, \ell'}^{(0)}(\psi_T) \right] \left(\frac{\partial \xi_{\ell'}}{\partial \psi_T}\right) + (\xi_{\ell'}) \left[- \frac{I}{(f + \epsilon I)} \left(\frac{d\epsilon}{d\psi_T}\right) \right. \\
 & \times (fm_{\ell'} + In) C_{\ell, \ell'}^{(0)}(\psi_T) - (\epsilon m_\ell - n)(m_{\ell'}) C_{\ell, \ell'}^{(1)}(\psi_T) - \frac{1}{(f + \epsilon I)} \left(\mu_0 \frac{dp}{d\psi_T}\right) (fm_{\ell'} + In) C_{\ell, \ell'}^{(2)}(\psi_T) + (\epsilon m_\ell - n) \\
 & \times (\epsilon m_{\ell'} - n) C_{\ell, \ell'}^{(4)}(\psi_T) - (\epsilon m_{\ell'} - n) C_{\ell, \ell'}^{(5)}(\psi_T) + \left. \frac{1}{(f + \epsilon I)} \left(\frac{d\epsilon}{d\psi_T}\right) (\epsilon m_{\ell'} - n) C_{\ell, \ell'}^{(6)}(\psi_T) \right] (\eta_{\ell'}) + (\eta_\ell) \\
 & \times \left[- \frac{I}{(f + \epsilon I)} \left(\frac{d\epsilon}{d\psi_T}\right) (fm_\ell + In) C_{\ell, \ell'}^{(0)}(\psi_T) + (\epsilon m_{\ell'} - n)(m_\ell) C_{\ell, \ell'}^{(1)}(\psi_T) - \frac{1}{(f + \epsilon I)} \left(\mu_0 \frac{dp}{d\psi_T}\right) (fm_\ell + In) C_{\ell, \ell'}^{(2)}(\psi_T) \right. \\
 & \left. - (\epsilon m_{\ell'} - n)(\epsilon m_\ell - n) C_{\ell, \ell'}^{(4)}(\psi_T) - (\epsilon m_\ell - n) C_{\ell, \ell'}^{(5)}(\psi_T) + \frac{1}{(f + \epsilon I)} \left(\frac{d\epsilon}{d\psi_T}\right) (\epsilon m_\ell - n) C_{\ell, \ell'}^{(6)}(\psi_T) \right] (\xi_{\ell'}) + (\eta_\ell) \\
 & \times \left. \left[\frac{1}{(f + \epsilon I)} (fm_\ell + In)(fm_{\ell'} + In) C_{\ell, \ell'}^{(0)}(\psi_T) + \frac{1}{(f + \epsilon I)} (\epsilon m_\ell - n)(\epsilon m_{\ell'} - n) C_{\ell, \ell'}^{(6)}(\psi_T) \right] (\eta_{\ell'}) \right\}, \quad (A1)
 \end{aligned}$$

where the poloidal contour integrals $C_{\ell, \ell'}^{(i)}(\psi_T)$ are

$$C_{\ell, \ell'}^{(0)}(\psi_T) = \frac{1}{2\pi} \int_{\theta_{\min}}^{\theta_{\max}} d\theta \cos[(m_\ell - m_{\ell'})\theta]; \quad (A2)$$

$$C_{\ell, \ell'}^{(1)}(\psi_T) = \frac{1}{2\pi} \int_{\theta_{\min}}^{\theta_{\max}} d\theta (\beta_*) \sin[(m_\ell - m_{\ell'})\theta]; \quad (A3)$$

$$C_{\ell, \ell'}^{(2)}(\psi_T) = \frac{1}{2\pi} \int_{\theta_{\min}}^{\theta_{\max}} d\theta (\sqrt{g}) \cos[(m_\ell - m_{\ell'})\theta]; \quad (A4)$$

$$C_{\ell, \ell'}^{(3)}(\psi_T) = \frac{1}{2\pi} \int_{\theta_{\min}}^{\theta_{\max}} d\theta (g_{\psi\psi} / \sqrt{g}) \cos[(m_\ell - m_{\ell'})\theta]; \quad (A5)$$

$$C_{\ell, \ell'}^{(4)}(\psi_T) = \frac{1}{2\pi} \int_{\theta_{\min}}^{\theta_{\max}} d\theta (g_{\psi\theta} / \sqrt{g}) \sin[(m_\ell - m_{\ell'})\theta]; \quad (A6)$$

$$C_{\ell, \ell'}^{(5)}(\psi_T) = \frac{1}{2\pi} \int_{\theta_{\min}}^{\theta_{\max}} d\theta \left(m_0 \frac{\vec{j} \cdot \vec{B}}{B^2} \right) \cos[(m_\ell - m_{\ell'})\theta]; \quad (A7)$$

$$C_{\ell, \ell'}^{(6)}(\psi_T) = \frac{1}{2\pi} \int_{\theta_{\min}}^{\theta_{\max}} d\theta (|\vec{\nabla}\psi_T|^2) \cos[(m_\ell - m_{\ell'})\theta]; \quad (A8)$$

$$C_{\ell, \ell'}^{(7)}(\psi_T) = \frac{1}{2\pi} \int_{\theta_{\min}}^{\theta_{\max}} d\theta [\partial(\sqrt{g}) / \partial \psi_T] \cos[(m_\ell - m_{\ell'})\theta]. \quad (A9)$$

APPENDIX B: 1D COMPRESSIBLE KINETIC PLASMA ENERGY

After the Fourier expansion (17)–(19) and integrating over θ , Eq. (20) becomes

$$\left(\frac{2}{4\pi^2} \delta W_k \right) = \frac{1}{2} \int_0^{\psi_T^{\text{edge}}} d\psi_T \rho_0(\psi_T) \sum_{\ell, \ell'} \left\{ \begin{array}{ll} (\xi_\ell) \left[K_{\ell\ell'}^{(1)}(\psi_T) + \frac{K_{\ell\ell'}^{(2)}(\psi_T)}{(f + \epsilon I)} \right] (\xi_{\ell'}) & + (\eta_\ell) \left[\frac{K_{\ell\ell'}^{(3)}(\psi_T) + [I(\psi_T)]^2 K_{\ell\ell'}^{(4)}(\psi_T)}{(f + \epsilon I)} \right] (\eta_{\ell'}) \\ + (\mu_\ell) [(f + \epsilon I) K_{\ell\ell'}^{(0)}(\psi_T)] (\mu_{\ell'}) & \\ + (\xi_\ell) \left[\frac{I(\psi_T) K_{\ell\ell'}^{(5)}(\psi_T) - K_{\ell\ell'}^{(8)}(\psi_T)}{(f + \epsilon I)} \right] (\eta_{\ell'}) & - (\eta_\ell) \left[\frac{I(\psi_T) K_{\ell\ell'}^{(5)}(\psi_T) - K_{\ell\ell'}^{(8)}(\psi_T)}{(f + \epsilon I)} \right] (\xi_{\ell'}) \\ - (\eta_\ell) [I(\psi_T) K_{\ell\ell'}^{(6)}(\psi_T)] (\mu_{\ell'}) & - (\mu_\ell) [I(\psi_T) K_{\ell\ell'}^{(6)}(\psi_T)] (\eta_{\ell'}) \\ - (\xi_\ell) [K_{\ell\ell'}^{(7)}(\psi_T)] (\mu_{\ell'}) & + (\mu_\ell) [K_{\ell\ell'}^{(7)}(\psi_T)] (\xi_{\ell'}) \end{array} \right\}, \quad (\text{B1})$$

where the poloidal contour integrals $K_{\ell\ell'}^{(i)}(\psi_T)$ are

$$K_{\ell\ell'}^{(0)}(\psi_T) = C_{\ell\ell'}^{(0)}(\psi_T); \quad (\text{B2})$$

$$K_{\ell\ell'}^{(1)}(\psi_T) = \frac{1}{2\pi} \int_{\theta_{\min}}^{\theta_{\max}} d\theta (\sqrt{g} |\vec{\nabla} \psi_T|^2) \cos[(m_\ell - m_{\ell'}) \theta]; \quad (\text{B3})$$

$$K_{\ell\ell'}^{(2)}(\psi_T) = \frac{1}{2\pi} \int_{\theta_{\min}}^{\theta_{\max}} d\theta (g[\beta_*^2 + \gamma_*^2 |\vec{\nabla} \psi_T|^2]) \cos[(m_\ell - m_{\ell'}) \theta]; \quad (\text{B4})$$

$$K_{\ell\ell'}^{(3)}(\psi_T) = \frac{1}{2\pi} \int_{\theta_{\min}}^{\theta_{\max}} d\theta (g |\vec{\nabla} \psi_T|^2) \cos[(m_\ell - m_{\ell'}) \theta]; \quad (\text{B5})$$

$$K_{\ell\ell'}^{(4)}(\psi_T) = \frac{1}{2\pi} \int_{\theta_{\min}}^{\theta_{\max}} d\theta (g) \cos[(m_\ell - m_{\ell'}) \theta]; \quad (\text{B6})$$

$$K_{\ell\ell'}^{(5)}(\psi_T) = \frac{1}{2\pi} \int_{\theta_{\min}}^{\theta_{\max}} d\theta (g \beta_*) \sin[(m_\ell - m_{\ell'}) \theta]; \quad (\text{B7})$$

$$K_{\ell\ell'}^{(6)}(\psi_T) = C_{\ell\ell'}^{(2)}(\psi_T); \quad (\text{B8})$$

$$K_{\ell\ell'}^{(7)}(\psi_T) = \frac{1}{2\pi} \int_{\theta_{\min}}^{\theta_{\max}} d\theta (\sqrt{g} \beta_*) \sin[(m_\ell - m_{\ell'}) \theta]; \quad (\text{B9})$$

$$K_{\ell\ell'}^{(8)}(\psi_T) = \frac{1}{2\pi} \int_{\theta_{\min}}^{\theta_{\max}} d\theta (g \gamma_* |\vec{\nabla} \psi_T|^2) \sin[(m_\ell - m_{\ell'}) \theta]. \quad (\text{B10})$$

APPENDIX C: 1D COMPRESSIBLE POTENTIAL PLASMA ENERGY

After the Fourier expansion (17)–(19) and integrating over θ , Eq. (21) becomes

$$\left(\frac{2}{4\pi^2} \delta W_p^c \right) = \frac{\Gamma}{2} \int_0^{\psi_T^{\text{edge}}} d\psi_T p(\psi_T) \sum_{\ell, \ell'} \left\{ \begin{array}{l} \left(\frac{\partial \xi_\ell}{\partial \psi_T} \right) [D_{\ell\ell'}^{(2)}(\psi_T)] \left(\frac{\partial \xi_{\ell'}}{\partial \psi_T} \right) + (\mu_\ell) [(\epsilon m_\ell - n)(\epsilon m_{\ell'} - n) D_{\ell\ell'}^{(6)}(\psi_T)] (\mu_{\ell'}) + \left(\frac{\partial \xi_\ell}{\partial \psi_T} \right) [D_{\ell\ell'}^{(3)}(\psi_T)] \\ \times (\xi_{\ell'}) + (\xi_\ell) [D_{\ell\ell'}^{(3)}(\psi_T)] \left(\frac{\partial \xi_{\ell'}}{\partial \psi_T} \right) + (\xi_\ell) [D_{\ell\ell'}^{(1)}(\psi_T)] (\xi_{\ell'}) + \left(\frac{\partial \xi_\ell}{\partial \psi_T} \right) [D_{\ell\ell'}^{(5)}(\psi_T) - m_{\ell'} D_{\ell\ell'}^{(2)}(\psi_T)] (\eta_{\ell'}) + (\eta_\ell) [-D_{\ell\ell'}^{(5)}(\psi_T) \\ - m_\ell D_{\ell\ell'}^{(2)}(\psi_T)] \left(\frac{\partial \xi_{\ell'}}{\partial \psi_T} \right) + (\xi_\ell) [D_{\ell\ell'}^{(7)}(\psi_T) - m_{\ell'} D_{\ell\ell'}^{(3)}(\psi_T)] (\eta_{\ell'}) + (\eta_\ell) [-D_{\ell\ell'}^{(7)}(\psi_T) - m_\ell D_{\ell\ell'}^{(3)}(\psi_T)] (\xi_{\ell'}) + (\eta_\ell) [D_{\ell\ell'}^{(4)}(\psi_T) \\ + m_\ell m_{\ell'} D_{\ell\ell'}^{(2)}(\psi_T) - (m_\ell - m_{\ell'}) D_{\ell\ell'}^{(5)}(\psi_T)] (\eta_{\ell'}) + (\mu_\ell) [(\epsilon m_\ell - n) D_{\ell\ell'}^{(8)}(\psi_T)] (\xi_{\ell'}) + (\xi_\ell) [(\epsilon m_{\ell'} - n) D_{\ell\ell'}^{(8)}(\psi_T)] (\mu_{\ell'}) \\ + (\mu_\ell) [(\epsilon m_\ell - n) D_{\ell\ell'}^{(0)}(\psi_T)] \left(\frac{\partial \xi_{\ell'}}{\partial \psi_T} \right) + \left(\frac{\partial \xi_\ell}{\partial \psi_T} \right) [(\epsilon m_{\ell'} - n) D_{\ell\ell'}^{(0)}(\psi_T)] (\mu_{\ell'}) + (\mu_\ell) [(\epsilon m_\ell - n) (D_{\ell\ell'}^{(9)}(\psi_T) - m_{\ell'} D_{\ell\ell'}^{(0)}(\psi_T))] \\ \times (\eta_{\ell'}) + (\eta_\ell) [(\epsilon m_{\ell'} - n) (-D_{\ell\ell'}^{(9)}(\psi_T) - m_\ell D_{\ell\ell'}^{(0)}(\psi_T))] (\mu_{\ell'}) \end{array} \right\}, \quad (\text{C1})$$

where the poloidal contour integrals $D_{\ell/\ell'}^{(i)}(\psi_T)$ are

$$D_{\ell/\ell'}^{(0)}(\psi_T) = C_{\ell/\ell'}^{(0)}(\psi_T); \quad (\text{C2})$$

$$D_{\ell/\ell'}^{(1)}(\psi_T) = \frac{1}{2\pi} \int_{\theta_{\min}}^{\theta_{\max}} d\theta \left[\frac{1}{\sqrt{g}} \left(\frac{\partial(\sqrt{g})}{\partial\psi_T} \right)^2 \right] \cos[(m_\ell - m_{\ell'})\theta]; \quad (\text{C3})$$

$$D_{\ell/\ell'}^{(2)}(\psi_T) = C_{\ell/\ell'}^{(2)}(\psi_T); \quad (\text{C4})$$

$$D_{\ell/\ell'}^{(3)}(\psi_T) = C_{\ell/\ell'}^{(7)}(\psi_T); \quad (\text{C5})$$

$$D_{\ell/\ell'}^{(4)}(\psi_T) = \frac{1}{2\pi} \int_{\theta_{\min}}^{\theta_{\max}} d\theta \left[\frac{1}{\sqrt{g}} \left(\frac{\partial(\sqrt{g})}{\partial\theta} \right)^2 \right] \cos[(m_\ell - m_{\ell'})\theta]; \quad (\text{C6})$$

$$D_{\ell/\ell'}^{(5)}(\psi_T) = \frac{1}{2\pi} \int_{\theta_{\min}}^{\theta_{\max}} d\theta \left(\frac{\partial(\sqrt{g})}{\partial\theta} \right) \sin[(m_\ell - m_{\ell'})\theta]; \quad (\text{C7})$$

$$D_{\ell/\ell'}^{(6)}(\psi_T) = \frac{1}{2\pi} \int_{\theta_{\min}}^{\theta_{\max}} d\theta \left(\frac{1}{\sqrt{g}} \right) \cos[(m_\ell - m_{\ell'})\theta]; \quad (\text{C8})$$

$$D_{\ell/\ell'}^{(7)}(\psi_T) = \frac{1}{2\pi} \int_{\theta_{\min}}^{\theta_{\max}} d\theta \left[\frac{1}{\sqrt{g}} \left(\frac{\partial(\sqrt{g})}{\partial\psi_T} \right) \left(\frac{\partial(\sqrt{g})}{\partial\theta} \right) \right] \times \sin[(m_\ell - m_{\ell'})\theta]; \quad (\text{C9})$$

$$D_{\ell/\ell'}^{(8)}(\psi_T) = \frac{1}{2\pi} \int_{\theta_{\min}}^{\theta_{\max}} d\theta \left[\frac{1}{\sqrt{g}} \left(\frac{\partial(\sqrt{g})}{\partial\psi_T} \right) \right] \cos[(m_\ell - m_{\ell'})\theta]; \quad (\text{C10})$$

$$D_{\ell/\ell'}^{(9)}(\psi_T) = \frac{1}{2\pi} \int_{\theta_{\min}}^{\theta_{\max}} d\theta \left[\frac{1}{\sqrt{g}} \left(\frac{\partial(\sqrt{g})}{\partial\theta} \right) \right] \sin[(m_\ell - m_{\ell'})\theta]. \quad (\text{C11})$$

¹A. H. Boozer, Phys. Fluids **24**, 1999 (1981).

²J. Nührenberg and R. Zille, in *Proceedings of the Workshop on Theory of Fusion Plasmas*, EUR 11336 EN (Editrice Compositori, Bologna, 1987), p. 3.

³P. C. Grim, J. M. Greene, and J. L. Johnson, in *Methods in Computational Physics* (Academic, New York, 1976), Vol. 16, p. 253.

⁴F. Rogier, G. Bracco, A. Mancuso, P. Micozzi, and F. Alladio, in *Proceedings of 11th International Congress on Plasma Physics*, ICPP 2002, Sydney, 2002, edited by I. S. Falconer, R. L. Dewar, and J. Khachan (American Institute of Physics, Melville, NY, 2003), Vol. 669, p. 557.

⁵J. B. Taylor and M. F. Turner, Nucl. Fusion **29**, 219 (1989).

⁶X. Z. Tang and A. H. Boozer, Phys. Plasmas **13**, 042514 (2006).

⁷F. Alladio, P. Costa, A. Mancuso, P. Micozzi, S. Papastergiou, and F. Rogier, Nucl. Fusion **46**, S613 (2006).

⁸F. Alladio, A. Mancuso, P. Micozzi, and F. Rogier, Phys. Plasmas **12**, 112502 (2005).

⁹I. B. Bernstein, E. A. Frieman, M. D. Kruskal, and R. M. Kulsrud, Proc. R. Soc. London, Ser. A **244**, 17 (1958).

¹⁰W. A. Cooper, Plasma Phys. Controlled Fusion **34**, 1011 (1992).

¹¹J. P. Freidberg, Rev. Mod. Phys. **54**, 801 (1982).

¹²M. S. Chu and P. B. Parks, Phys. Plasmas **11**, 4859 (2004).

¹³R. Gruber and J. Rappaz, *Finite Element Methods in Linear Ideal Magnetohydrodynamics* (Springer-Verlag, Berlin, 1985), p. 39.

¹⁴L. Degtyarev, A. Martynov, S. Medvedev, F. Troyon, L. Villard, and R. Gruber, Comput. Phys. Commun. **103**, 10 (1997).

¹⁵P. M. Morse and H. Feshbach, *Methods of Theoretical Physics* (McGraw-Hill, New York, 1953), p. 1797.

¹⁶M. S. Chance, Phys. Plasmas **4**, 2161 (1997).